

## Chapter 2

# Type Synthesis of Parallel Mechanisms

**Abstract** This chapter presents several general methods to achieve type synthesis of parallel mechanisms. In particular, an evolution-based approach is used for type synthesis and comprehensive enumeration of parallel mechanisms with parallelogram, as given the number of DOF ranging from 1 to 6. A number of novel mechanical architectures can be obtained correspondingly to improve the kinematic performances of traditional parallel mechanisms. Representative types of parallel mechanisms will then be chosen to be studied more specifically in the remainder of this book.

**Keywords** Architectures • Type synthesis • DOF analysis • Parallel mechanism • Evolution • Parallelogram

### 2.1 DOF Analysis

In this chapter, we consider a parallel mechanism to have  $n$  DOFs. That is, the mechanism has  $n$  DOFs in its normal configuration, excluding any singularity. The mechanism may lose or gain one or more DOFs in its singularity. This will be discussed in detail in Chap. 5.

Perhaps the foremost concern in studying the kinematics of mechanisms is the number of DOFs. The DOF of a mechanism is the number of independent parameters or input needed to completely specify the configuration of the mechanism. However, defining a general mobility criterion for closed-loop kinematic chains is difficult, as Hunt (1978) and Lerbet (1987) noted. Classical mobility formulas can cause the disregard of some DOFs. Grübler-Kutzbach's formula (Kutzbach 1933) is nevertheless generally used, and it may be written as

$$M = d(n - g - 1) + \sum_{i=1}^g f_i \quad (2.1)$$

where

$M$ : the mobility (DOFs of a system)

$d$ : the order of the screw system that applies ( $d = 3$  for planar and spherical motion,  $d = 6$  for spatial motion)

$n$ : the number of links including the frame

$g$ : the number of joints

$f_i$ : the DOFs associated with the  $i$ th joint

We can calculate the DOF number of a mechanism using Eq. (2.1). Nevertheless, this equation is not the universal equation for all parallel mechanisms. Sometimes, it fails when it is applied to a parallel mechanism with excessive constraints. For example, when it is applied to Tsai's mechanism (Fig. 1.23), it yields  $M = -3$ .

To precisely calculate the number of DOFs of a parallel mechanism, many scholars elaborated on Eq. (2.1) or proposed a new criterion. In 2003, Huang and Li (2003) provided a DOF criterion for some lower mobility parallel mechanisms with closed loops in each of their legs using constraint analysis to aid DOF analysis by the Grübler-Kutzbach's formula. In 2005, Gogu (2005) provided a brief presentation and conducted critical analysis of 35 approaches/formulas presented in literature during the last 150 years for DOF calculation and their origins, similarities, and limitations. In his article, he also explained why these formulas do not work for certain mechanisms and proposed a new formula for the rapid DOF calculation of parallel mechanisms with elementary legs. Dai et al. (2006) have recently presented a DOF criterion for overconstrained parallel platforms that employ both screws and reciprocal screws. Rico et al. (2006) proposed a criterion based on an analysis of the subalgebras of Lie algebra,  $se(3)$ , also known as screw algebra, of the Euclidean group,  $SE(3)$ . The criterion is said to provide the correct number of DOFs for a wider class of parallel mechanisms.

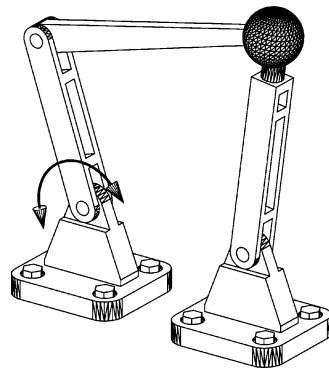
However, the objective of DOF analysis is never the DOF number itself, but both the DOF number and type, i.e., how many DOF numbers are there and what kind are they classified under. These targets indicate that the DOF formula is far from perfect. DOF analysis based on screw theory and Lie algebra may provide both the DOF number and type. Here, we introduce some methods of DOF analysis without the use of any mathematics.

### 2.1.1 Observation Method

This method can be applied to the DOF analysis of simple parallel mechanisms, some parallel mechanisms with a passive leg, and parallel mechanisms with six DOFs.

In the DOF analysis of a mechanism, the joint is the most important component. The observation method is based on the comprehensive understanding of the free motion of a joint. For example, with an R joint, the link may only rotate about the

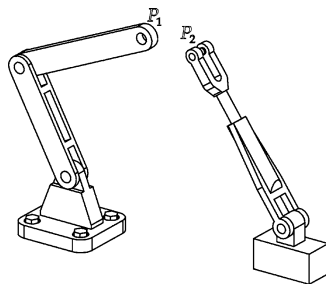
**Fig. 2.1** RRSR four-bar mechanism



joint axis and remain in a specified plane; any point at the link describes a circle path centered at the point on the joint axis. If a link is linked to another by a prismatic joint, the loci of all the points at the link are straight lines that are parallel to one another. With a spherical joint, the link can rotate with respect to any line passing through the center of the joint.

Let us first consider planar parallel mechanisms. Only a 1-DOF joint normally exists in a planar parallel mechanism. For a planar mechanism with multi-DOF joints, one or more DOFs of the joint will lose its motion function but will play a mechanical role (e.g., guaranteeing the free motion of the mechanism if an error or deformation occurs). In this case, we say that there is an idle (or passive) DOF in the mechanism. A four-bar mechanism with an RRSR chain is shown in Fig. 2.1. Kinematically, only one DOF of the spherical joint is effective; the remaining two DOFs are idle. With the S joint, the planar four-bar mechanism still has one DOF. However, idle DOFs are necessary in some machines, especially in heavy machines (e.g., the heavy forming machine that works under a very large payload). In this chapter, we consider only the parallel mechanism without idle DOFs.

Revolute and prismatic joints are typically used in a planar parallel mechanism (see Figs. 1.12, 1.13, 1.15, and 1.16). The observation of the RRRPR parallel mechanism in Fig. 1.12b shows that it consists of two legs, i.e., the RR and RP chains, which are connected together by a common revolute joint, referred to as the end-effector of the mechanism. Our concern is the DOF of this end-effector. Because reference points  $P_1$  and  $P_2$  (Fig. 2.2) of the RR and RP chains have the same DOFs, i.e., two translational DOFs in the  $O$ - $xy$  plane, the end-effector of the RRRPR parallel mechanism has the two DOFs. Similarly, we may infer that the end-effectors of the other parallel mechanisms shown in Fig. 1.12 have two translational DOFs. Given that the end-effector (the mobile platform) of each parallel mechanism shown in Figs. 1.15 and 1.16 is connected to the base by three planar kinematic chains, each mechanism consists of three single-DOF joints. The end-effector of such a chain has three DOFs in a plane. Any leg of the parallel mechanisms imposes no kinematic constraint on two others; thus, their mobile platforms have three DOFs, i.e., two translations and one rotation in a plane.

**Fig. 2.2** RR and RP chains

Now, we consider the mechanism shown in Fig. 3.2c. The mobile platform of the mechanism is connected to the base by the RRR and PRRR chains. The axes of the RRR chains are all parallel to the others and are orthogonal to those in the PRRR chains. This arrangement shows that with the RRR chain, the mobile platform has three planar DOFs, i.e., two translations in the  $O$ - $xy$  plane and one rotation about the  $z$ -axis. However, the rotation is constrained by the PRRR chain. Therefore, the mobile platform has only two translational DOFs.

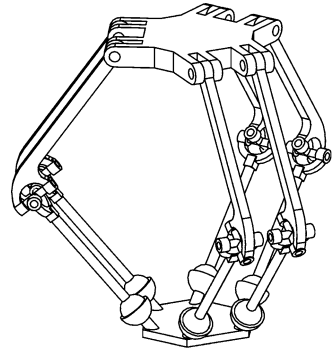
In the family of parallel mechanisms, some mechanisms with  $n$  DOFs usually consist of  $n$  identical actuated legs with six DOFs and one passive leg with  $n$  DOFs connecting the mobile platform and base. This means that the DOF of the mechanism is dependent on the DOF of the passive leg. Such a mechanism has an advantage: its rigidity can be improved through optimization of the link rigidities to reach maximal global stiffness and precision (Zhang and Gosselin 2002). The Tricept parallel mechanism (Fig. 1.29b) is such a mechanism. In the Tricept, the fourth leg is a UP chain, which has two rotational DOFs and one translational DOF. Therefore, the parallel mechanism has the said DOFs, and identifying the DOFs of this group of parallel mechanisms is very easy.

The end-effector of a 6-DOF chain has six DOFs, i.e., three translations and three rotations. If the mobile platform (not an end point) is connected to the base through several 6-DOF chains, the platform is guaranteed to have six DOFs. If the chain number equals six, one DOF in each leg is actuated; if the number is less than six, at least one leg will have more than one actuator. Thus, analyzing the DOF of a parallel mechanism that has all 6-DOF chains may be the easiest approach.

### 2.1.2 Evolution Method

DELTA has achieved significant success in industry because of its rapid performance and easy setup. The mechanism itself, however, seems complex. An issue is how many DOFs DELTA has, or why it has three translational DOFs when it is first encountered. Perhaps the design conceived by Clavel for DELTA did not originate from the 6-DOF parallel mechanism. If we assume such an origin, the DOF analysis of DELTA will be easy. Figure 2.3 shows Pierrot's 6-DOF parallel mechanism with

**Fig. 2.3** Pierrot's 6-DOF parallel mechanism (Pierrot et al. 1991)



six RUS chains (Pierrot et al. 1991), in which every two legs are parallel to each other when the mechanism is in its initial configuration. If the input of two parallel legs is the same at every moment, the DOFs of the mobile platform are therefore three translations. In this case, the two parallel input links can be replaced with a single link and six actuators become three. The modified mechanism is DELTA, indicating that DELTA has three pure translational DOFs in space.

This DOF analysis method is useful only if the original mechanism of a parallel mechanism can be found. Sometimes, this is not an easy task.

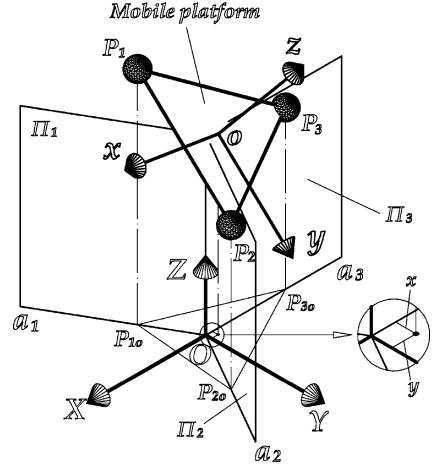
### 2.1.3 Kinematic Analysis Method

Some mechanisms such as the 3-[PP]S parallel mechanisms shown in Fig. 1.20 have complex kinematic chains. Completely identifying the DOFs of these mechanisms is impossible using the methods mentioned above. For example, the mechanism in Fig. 1.20a has three RPS chains, each with five DOFs, i.e., two translations and three rotations. This kind of kinematic chain has one less DOF than the PRPS chain of the mechanism in Fig. 1.38a, which has six actuators in three legs and six DOFs. On this basis, we can conclude that the 3-PRS mechanism has three DOFs. However, we cannot identify exactly what the DOFs are. To this end, we can first analyze its kinematics by assuming that the mobile platform has six DOFs.

Figure 2.4 illustrates the kinematic model of a 3-[PP]S mechanism, in which points  $P_1$ ,  $P_2$ , and  $P_3$  of the mobile platform remain at planes  $\Pi_1$ ,  $\Pi_2$ , and  $\Pi_3$ , respectively. The three points can be connected to the base by any one of the RR, RP, PR, and PP chains or other chains similar to these.

A kinematic model of the mechanism is developed, as shown in Fig. 2.4. The vertices of the output platform are denoted as platform joints  $P_i$  ( $i = 1, 2, 3$ ), and the vertices of the base joints are denoted as  $B_i$  ( $i = 1, 2, 3$ ). A fixed global reference system  $\mathfrak{R}$ :  $O$ -XYZ is located at the intersecting point of three planes  $\Pi_1$ ,  $\Pi_2$ , and  $\Pi_3$  with the  $z$ -axis coincident with the intersecting line and  $x$ -axis in plane  $\Pi_3$ . Another reference frame, called moving frame  $\mathfrak{R}'$ :  $o$ -xyz, is located at the center

**Fig. 2.4** Kinematic model of a 3-[PP]S mechanism



of regular triangle  $P_1 P_2 P_3$ . The  $z$ -axis is perpendicular to mobile platform  $P_1 P_2 P_3$ ,  $x$ -axis directed along the  $P_3 o$  direction, and  $y$ -axis in the mobile platform.

We assume that the mobile platform has six DOFs. Its pose is represented by a vector  $X = [x \ y \ z \ \psi \ \theta \ \phi]^T$ , where  $\psi$ ,  $\theta$ , and  $\phi$  are three Euler angles. The position of the mobile platform in frame  $\mathfrak{N}$  is given by the position vector  $(o)_{\mathfrak{N}}$  of point  $o$  and the orientation given by matrix  $T$ . Moreover, there are

$$(o)_{\mathfrak{N}} = [x \ y \ z]^T \quad (2.2)$$

$$\begin{aligned} T &= T_{ZXY} = R_Y(\theta) R_X(\psi) R_Z(\phi) \\ &= \begin{bmatrix} c_\theta c_\phi + s_\psi s_\theta s_\phi & -c_\theta s_\phi + s_\psi s_\theta c_\phi & c_\psi s_\theta \\ c_\psi s_\phi & c_\psi c_\phi & -s_\phi \\ -s_\theta c_\phi + s_\psi c_\theta s_\phi & s_\theta s_\phi + s_\psi c_\theta c_\phi & c_\psi c_\theta \end{bmatrix} \end{aligned} \quad (2.3)$$

where  $c$  stands for cosine and  $s$  for sine. Vectors  $(P_i)_{\mathfrak{N}'}$  are defined as the position vectors of points  $P_i$  in frame  $\mathfrak{N}'$ , and

$$(P_i)_{\mathfrak{N}'} = [P'_{ix} \ P'_{iy} \ P'_{iz}]^T = [r \cos \varphi_i \ r \sin \varphi_i \ 0]^T \quad (2.4)$$

where  $\varphi_i = (i - 1) 2\pi / 3$  and  $r$  is the radius of the mobile platform. Then, the position vectors of points  $P_i$  in frame  $\mathfrak{N}$  can be written as

$$(P_i)_{\mathfrak{N}} = [P_{ix} \ P_{iy} \ P_{iz}]^T = T (P_i)_{\mathfrak{N}'} + O' \quad (2.5)$$

That is,

$$P_{ix} = x + T_{11}P'_{ix} + T_{12}P'_{iy} + T_{13}P'_{iz} \quad (2.6)$$

$$P_{iy} = y + T_{21}P'_{ix} + T_{22}P'_{iy} + T_{23}P'_{iz} \quad (2.7)$$

$$P_{iz} = z + T_{31}P'_{ix} + T_{32}P'_{iy} + T_{33}P'_{iz} \quad (2.8)$$

where  $T_{jk}(j, k = 1, 2, 3)$  is the  $j$ th row and  $k$ th column element in matrix  $T$ .

Figure 2.4 shows that each point of  $P_i$  ( $i = 1, 2, 3$ ), which are vertices of the mobile platform, is always in a fixed plane. Therefore, we can write three constraint equations as follows:

$$P_{1y} = 0 \quad (2.9)$$

$$P_{2y} = -\sqrt{3} P_{2x} \quad (2.10)$$

$$P_{3y} = \sqrt{3} P_{3x}. \quad (2.11)$$

That is,

$$y + T_{21}r = 0 \quad (2.12)$$

$$y - \frac{r}{2}T_{21} + \frac{\sqrt{3}r}{2}T_{22} = -\sqrt{3}x + \frac{\sqrt{3}r}{2}T_{11} - \frac{3r}{2}T_{12} \quad (2.13)$$

$$y - \frac{r}{2}T_{21} - \frac{\sqrt{3}r}{2}T_{22} = \sqrt{3}x - \frac{\sqrt{3}r}{2}T_{11} - \frac{3r}{2}T_{12}. \quad (2.14)$$

From Eqs. (2.12), (2.13), and (2.14), we can obtain the following equations:

$$T_{21} = T_{12} \quad (2.15)$$

$$x = \frac{r}{2} (T_{11} - T_{22}). \quad (2.16)$$

Equations (2.12), (2.15), and (2.16) can be rewritten as

$$y = -rc_{\psi}s_{\phi} \quad (2.17)$$

$$-c_{\theta}s_{\phi} + s_{\psi}s_{\theta}c_{\phi} - c_{\psi}s_{\phi} = 0 \quad (2.18)$$

Then,

$$\phi = \tan^{-1} \left[ \frac{s_\psi s_\theta}{(c_\psi + c_\theta)} \right] \quad (2.19)$$

$$x = \frac{r}{2} (c_\theta c_\phi + s_\psi s_\theta s_\phi - c_\psi c_\phi). \quad (2.20)$$

We can conclude that in vector  $\mathbf{X} = [x \ y \ z \ \psi \ \theta \ \phi]^T$ , only  $z$ ,  $\psi$ , and  $\theta$  are independent, and three others,  $x$ ,  $y$ , and  $\phi$ , are dependent on  $\psi$  and  $\theta$ . That is, a 3-[PP]S parallel mechanism has three independent DOFs, which are the translation along the Z-axis and two rotations about the X- and Y-axes.

However, these three methods cannot be applied to the DOF analysis of any parallel mechanism. The successful identification of DOF number and type can be implemented using screw theory or Lie algebra.

### 2.1.4 Method Based on Screw Theory

In the screw theory (Ball 1900), a unit screw  $\mathcal{S}$  is defined by a straight line with an associated pitch, as illustrated in Fig. 2.5, and is expressed as in a Plücker coordinate form

$$\mathcal{S} = (s; s^0) = (s; s_0 + ps) = (s; \mathbf{r} \times s + ps) \quad (2.21)$$

where  $s$  is a unit vector pointing in the direction of the screw axis,  $s_0 = \mathbf{r} \times s$  defines the moment of the screw axis about the origin of a reference frame,  $\mathbf{r}$  is the position vector of any point on the screw axis with respect to the reference frame, and  $p$  is the pitch of the screw. If  $p$  is equal to zero, the screw reduces to

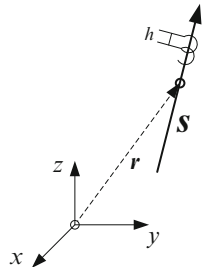
$$\mathcal{S} = (s; s_0) = (s; \mathbf{r} \times s) \quad (2.22)$$

On the other hand, if  $p$  is infinite, the screw can be defined as

$$\mathcal{S} = (0; s) \quad (2.23)$$

The screw expressed by Eq. (2.22) can represent a rotation in kinematics or a force in statics, and the screw expressed by Eq. (2.23) can represent a translation in kinematics and a couple in statics. We call the screw a twist if it represents the instantaneous rotation or translation of a rigid body and a wrench if it denotes a force or couple acting on a rigid body. In this regard, the first three components of a twist represent the unit angular velocity, and the last three components represent the unit linear velocity of a point in the rigid body that is instantaneously coincident with



**Fig. 2.5** A general screw

the origin of a reference frame. In similar, the first three components of a wrench represent the unit resultant force, and the last three components represent the unit resultant moment about the origin of a reference frame. A wrench of zero pitch represents a pure force, whereas a wrench of infinite pitch denotes a pure couple. On the other hand, a revolute joint can be represented by the screw expressed by Eq. (2.22), and a prismatic joint can be represented by the screw expressed by Eq. (2.23).

A unit screw,  $\$^r = (s^r; s^{0r})$ , and a set of unit screws,  $\$, \$_2, \dots, \$_n$ , are said to be reciprocal if they satisfy the condition

$$\$^r \circ \$_i = s_i \cdot s^{0r} + s_i^0 \cdot s^r = 0 \quad (i=1, 2, \dots, n) \quad (2.24)$$

where “ $\circ$ ” represents the reciprocal product and  $\$_i$  is the  $i$ th screw of the screw set.

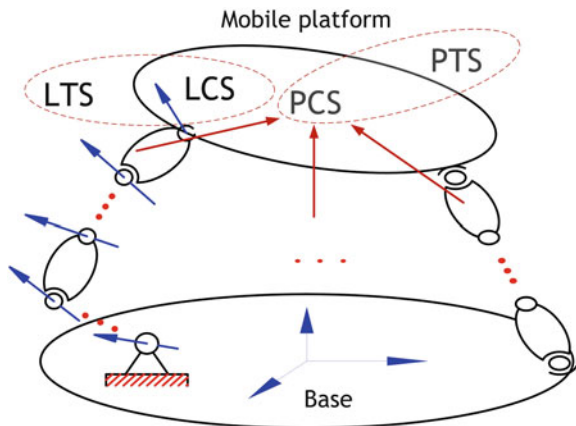
In an  $n$ -DOF serial manipulator, the twists associated with all the joints form a screw system of order  $n$ , called an  $n$ -system, provided that all the joint screws are linearly independent. For a spatial manipulator, if  $n = 6$ , there exists no screw reciprocal to the twist screw system. If  $n < 6$ , there exists  $6-n$  linearly independent wrenches that form a  $(6-n)$ -system. Each wrench in the  $(6-n)$ -system is reciprocal to the  $n$ -system of twists, namely,

$$\$_j^r \circ \$_i = 0 \quad (i=1, 2, \dots, n \text{ and } j=1, 2, \dots, 6-n) \quad (2.25)$$

Equation (2.25) can be used to solve for a  $(6-n)$ -system of reciprocal wrenches. On the other hand, given  $6-n$  linearly independent wrenches, Eq. (2.25) can be used to find an  $n$ -system of twists.

For a parallel manipulator illustrated in Fig. 2.6, when each kinematic pair in a limb is expressed as a unit screw, all these unit screws form a *limb twist system* (LTS). The linearly independent joint screws of a limb form an  $n$ -system. The reciprocal screws form a  $(6-n)$ -system, called a *limb wrench system* or a *limb constraint system* (LCS). In a low-DOF parallel manipulator, we note that a single limb exerts some restrictions on the moving platform. The overall constraint imposed on the moving platform, which is called a *platform wrench system* or a *platform constraint system* (PCS), is obtained by a combination of all LCSs. The PCS represents the restricted DOFs of the moving platform. Thus, the DOF

**Fig. 2.6** Several pairs of screw systems in parallel mechanisms



of the moving platform can be determined by the *platform twist system* (PTS), which is reciprocal to the manipulator constraint system. In other words, the motion characteristics of the moving platform are completely determined by the nature of the PCS. For instance, for a general 3-DOF translational parallel manipulator (TPM), the PCS consists of three linearly independent constraint couples:

$$\begin{aligned} \mathcal{S}_1^c &= (0\ 0\ 0; 1\ 0\ 0) \\ \mathcal{S}_2^c &= (0\ 0\ 0; 0\ 1\ 0) \\ \mathcal{S}_3^c &= (0\ 0\ 0; 0\ 0\ 1) \end{aligned} \quad (2.26)$$

which restricts three rotations of the moving platform (Fig. 2.6).

In general, when using the method based on the screw theory to determine the degrees of freedom of a low-DOF parallel manipulator, a whole analysis procedure is described as follows. First, select a single limb from the parallel manipulator. For the purpose of a convenient analysis, all multiple-DOF pairs in this limb are deposited into the equivalent basic joints. Thus, these 1-DOF kinematic pairs in the limb form a LTS. Next, an LCS reciprocal to the LTS, representing the constraint forces or couples acting on the moving platform, is derived by means of Eq. (2.25). In similar, the constraint forces or constraint couples provided by the other limbs are also obtained. All these derived screws compose a PCS, which represents the overall constraints for the parallel manipulator. Finally, by calculating the reciprocal product of the PCS, a PTS reflecting all instantaneous motions of this manipulator is obtained, and the DOF of the manipulator is determined accordingly.

Therefore, in order to achieve the type synthesis of a class of parallel manipulators, the process described above can provide us with a good inspiration. In other words, the screw theory is still effective during the synthesis process. The concrete synthesis process is realized through the following steps:

*Step 1: Describe all constraint screws acting on the movable platform.*

For any TPM, its moving platform has only three-dimensional translations and loses three rotational DOFs; thus, there exist three linearly independent CCs acting on the moving platform. These three constraint couples form a PCS of the TPMs, as described in Eq. (2.26).

*Step 2: Analyze the geometric condition of the LCS corresponding to a specific PCS.*

Different PCSs in a parallel manipulator result from the combination of all the LCS under different geometric conditions. In this sense, it is very necessary to analyze the geometric condition of the LCS corresponding to a specific PCS in order to obtain an available limb structure.

The family of the TPMs can be grouped into two categories: manipulators with independent constraints and manipulators with repeated constraints (also called overconstrained manipulators). In an overconstrained manipulator, its limb has less than five basic joints, which means fewer joints and simpler architecture than an independent-constraint manipulator with the same kinematic characteristics. In this regard, by analyzing the geometric condition of the LCS in terms of TPMs with independent constraints and overconstrained TPMs, respectively, we can find the corresponding PCS.

*Step 3: Make a solution to the LTS reciprocal to the LCS.*

According to the screw theory, each of screws in a LTS is reciprocal to the LCS. Therefore, once the screws in the LCS given, the screws in the LTS can be calculated by means of Eq. (2.25). A simple approach of determining a LTS is to find a base of this LTS. Then by a linear combination of these basic twists, other types of the LTS reflecting the limb structure can be obtained.

*Step 4: Analyze the geometric condition of the LTS corresponding to different LCS.*

In a TPM, each limb may provide couples with different numbers varied from zero to three to the moving platform; therefore, we should analyze the geometric condition met by the LTS corresponding to any kind of LCS such that we can find the geometric relationship among all kinematic pairs in the LTS and further construct this limb. Furthermore, to make sure that the moving platform could achieve a finite motion instead of an instantaneous motion, the arrangement of the kinematic pairs in each limb has to meet some additional geometric conditions, which is an important issue to be discussed.

*Step 5: Construct and allocate available the connecting chains in series.*

Once we have obtained the LTS satisfying some geometric conditions, we can construct a limb according to the screw expressions reflecting this LTS. On the other hand, note that the sequence of each screw in the LTS is changeable, which means the arrangement of the kinematic pairs may also be alterable.

*Step 6: Construct a desired parallel mechanism according to Steps 2–5.*

## 2.2 Evolution of Parallel Mechanisms

In the field of parallel mechanisms, an interesting problem is the identification of a method for designing a mechanical architecture for a parallel mechanism being given its number and type of DOF. After Gough established the basic principles of a mechanism with a closed-loop kinematic structure in 1947, many other parallel mechanisms with a specified DOF number and type have also been proposed. However, some parallel mechanisms have inherent relationships with others. A parallel mechanism may have evolved from another. We introduce the typical evolution of parallel mechanisms. As mentioned in Sect. 3.2.2, the evolution of parallel mechanisms may help us identify their DOFs.

Figure 1.36 shows the general architecture of 6-DOF parallel mechanisms. Theoretically, the arrangement of the six legs of the mechanism can be done at will, which leads to some potential 6-DOF parallel mechanisms, such as the mechanism shown in Fig. 1.37b, in which the legs are arranged in 3.2.1 style. This architecture presents application advantages in a micromotion system (Pernette and Clavel 1996) and shake table. The disposal of six legs (as shown in Fig. 1.37c, d) causes the mechanisms to move freely along a specified direction; this feature is very useful in industrial applications (Honegger et al. 2000).

Applying parallelity between every two legs of the six-leg mechanism in Fig. 1.36 generates the 6-DOF parallel mechanism presented in Fig. 1.37a. The number of DOFs of the mechanism differs if the two most adjacent legs have identical input. This is a topological mechanism of DELTA with linear actuators. Replacing the active P joints of the mechanism in Fig. 1.37a with R joints and fixing them to the base result in the modified mechanism with revolute actuators presented by Pierrot (1991; Fig. 2.3). Similarly, the mechanism can evolve to a DELTA robot. The fact that the two nearby revolute actuators in Fig. 2.3 always have the same output generates a different mobile platform output. This feature characterizes the design of the well-known DELTA robot (Fig. 1.22).

The supposed design conceived for the above-mentioned mechanisms not only aids the understanding of the mechanisms but also provides us new concepts for the design of a mechanism. For example, the 6-DOF parallel mechanism (Fig. 2.7) described in Dafaoui et al. (1998) can be taken as the topological architecture of the mechanism shown in Fig. 1.37a by rearranging the six legs. This inspires the design of new parallel mechanisms (see Fig. 1.26a, b) through the rearrangement of the three legs of DELTA and Tsai's parallel mechanism. In the two new designs, the three actuators are arranged according to the Cartesian axes, indicating that the actuation directions are normal to one another. In addition, the joints connected to the mobile platform are located on three sides of a cube; for this reason, we call this type of mechanism the parallel cube-mechanism. The mechanisms also have three translational DOFs, as in the cases of DELTA and Tsai's mechanism. However, some of their important characteristics differ from those of DELTA and Tsai's mechanism, making the designs novel. One of the most important study results of Liu et al. (2003) shows that a compliance center exists in the workspace,

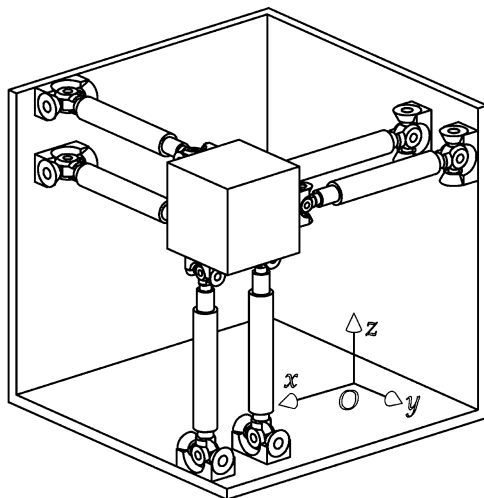


**Fig. 2.7** Six-DOF parallel cube-mechanism with six UPS chains

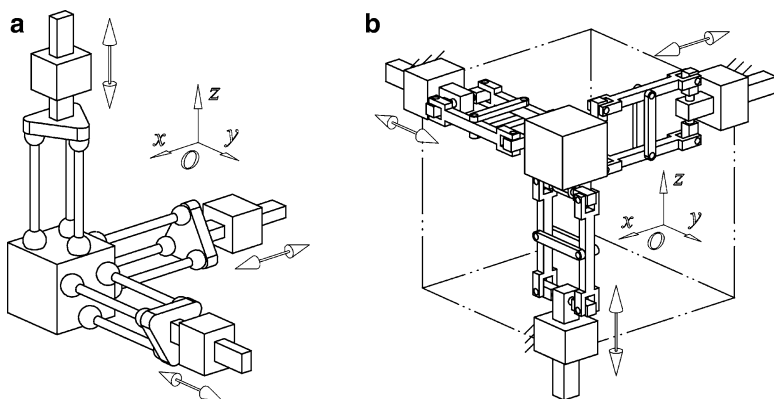
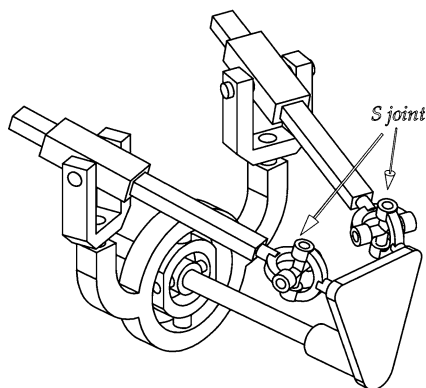


**Fig. 2.8** Two pure translational parallel cube-mechanisms (Liu et al. 2003) with redundant constraint: (a) modification of DELTA and (b) modification of Tsai's mechanism

which is the initial position. At this point, the parallel cube-mechanisms behave in a manner similar to both a velocity and stiffness isotropic setup. These characteristics make the parallel cube-mechanism adaptive to such applications as micromotion mechanisms (Liu et al. 2001b; Ohya et al. 1999), remote center compliance devices (Kim et al. 1997), precision assembly machines (Dafaoui et al. 1998), and parallel kinematic machines (Huang et al. 2002). For application in a parallel kinematic machine, the stiffness of the system is one of the most important problems. The advantage of the presented parallel mechanisms is that the stiffness can be improved by increasing the redundant constraints (Liu et al. 2003), as in the architectures shown in Fig. 2.8. Figure 2.8a shows the modified version of the design in Fig. 3.14a,

**Fig. 2.9** Three-DOF parallel mechanism with 2-UPS&1-UP chains (the parallel mechanism of TriVariant (Huang et al. 2005a))



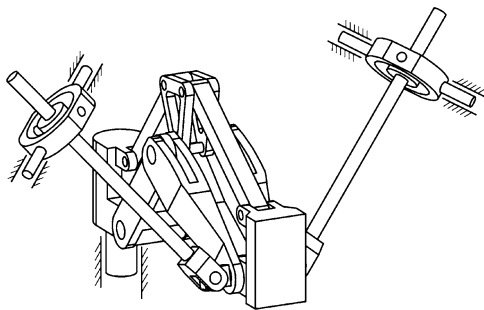
in which there are three spherical-bar-spherical or universal-bar-universal chains instead of two such chains in each leg. As seen in Fig. 2.8b, each parallelogram in Fig. 1.26b is divided into two or more parallelograms. The kinematic model of each of the mechanisms is identical to that of each of the mechanisms shown in Fig. 1.26. Furthermore, the revision has no negative influence on the kinematics, workspace, and other performance-related functions of the mechanism. The more redundant the constraint of the leg, the higher the stiffness of the mechanism and, in relative terms, the higher the fabrication accuracy it requires.

As shown in Fig. 1.29b, the parallel mechanism of the Tricept is equipped with the 3-UPS&1-UP chains, in which the P joints of the three UPS chains are active and the P joint of the UP chain is passive. On the basis of this mechanism, Huang and colleagues (2005a) designed a modified version with 2-UPS&1-UP chains (see Fig. 2.9), in which the three P joints are all active. Using this mechanism, Tianjin University (China) developed a 5-DOF hybrid machine called TriVariant. The modification not only inherits most of the advantages of the Tricept but also allows for cost-effectiveness compared with the Tricept because of the savings gained from forgoing one active limb. As analyzed in Huang et al. (2005a), the kinematic performance of TriVariant is comparable with that of the Tricept for the same task workspace and a set of similar geometrical parameters.

Again, considering the SKM 400 parallel mechanism shown in Fig. 1.29d, three P joints in the UPS chains are active, but the R joint in the R(Pa)(Pa) leg is passive. A 3-DOF pure translational parallel mechanism was proposed (Huang et al. 2005b), in which one UPS leg from the SKM 400 mechanism is excluded and the R joint is actuated (Fig. 2.10).

Although the design concepts from so many parallel mechanisms provide us more concepts for the design of a new mechanism, additional work remains to be done especially for designing lower-DOF parallel mechanisms that combine translational and rotational DOFs. Few spatial three-DOF parallel mechanisms combine two spatial translations and one rotation; these are presented in the following chapter.

**Fig. 2.10** Three-DOF pure translational parallel mechanism with 2-UPS&1-R(Pa)(Pa) chains (Huang et al. 2005b)



## 2.3 Type Synthesis

In the field of parallel mechanisms, one of the most important and interesting problems is architecture design, i.e., type synthesis. Numerous parallel mechanisms with a specified number and type of DOF have been proposed (see Merlet (2000) for examples). Most recently, several systematic approaches have been proposed for the type synthesis of parallel mechanisms, such as the methods based on displacement group theory (Hervé 1999) and screw theory (Zhao 2000; Huang and Li 2002; Fang and Tsai 2002; Kong and Gosselin 2004a, b), as well as the units of single opened chains (Yang 2004), vector approach (Carricato and Parenti-Castelli 2003), and Lie subgroups and submanifolds of the special Euclidean group, SE(3) (Meng et al. 2007). Using these methods as bases, researchers proposed many new parallel mechanisms that have not been previously conceived of. These substantially enrich the theory of parallel mechanisms. In this paper, we introduce the type synthesis of some parallel mechanisms.

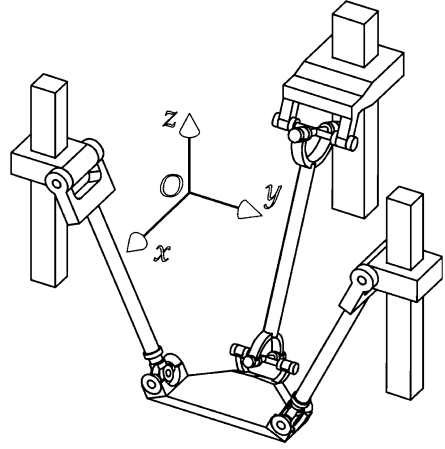
### 2.3.1 Type Synthesis of Parallel Mechanisms with Parallelogram

#### 2.3.1.1 Motivation

Few spatial parallel mechanisms with two translations and one rotation exist in the family of parallel mechanisms, and few fully parallel mechanisms have high rotational capability. To these ends, we design a mechanism that satisfies these requirements.

Equation (2.1) indicates that in a symmetrical spatial parallel mechanism, each of the three legs should have five DOFs. The 3-PRS parallel mechanism is a typical example. Then, we consider the mechanism shown in Fig. 2.11, in which the mobile platform is connected to the base through two PRS chains and one PUU chain.

**Fig. 2.11** Parallel mechanism with a 2-PRS&1-PUU chain



In this design, the R joints of two PRS legs are parallel to each other, and the legs are in a common plane. With this architecture, the mechanism should have three DOFs. With the two PRS legs, the mobile platform cannot move along the  $x$ -axis and cannot rotate about the  $z$ -axis, leaving four DOFs, two translations, and two rotations on the mobile platform. For example, endowing the mobile platform with three spatial DOFs necessitates two translations and one rotation; the third leg with the PUU chain must constrain the rotational DOF of the mobile platform about the  $x$ -axis. Whether this can be accomplished depends on the UU chain. A question arises as to the ability of the UU chain to constrain the rotational DOF. To resolve this issue, we first investigate the kinematic characteristics of the UU chain.

Figure 2.12a shows a UU chain, in which the axes of four revolute joints are denoted as  $y_1$ ,  $z_1$ ,  $y_2$ , and  $z_2$ . At any moment, the  $y_1$ -axis is always parallel to the  $y_2$ -axis. The configuration when links 1, 2, and 3 are collinear is referred to as the initial configuration. In this chain, there are four DOFs that are four rotations about the four axes. In movement, if the  $z_1$ -axis is always parallel to the  $z_2$ -axis, we call this translational motion; otherwise, it is referred to as spatial motion. In translational motion, axes  $y_1$  and  $y_2$  and axes  $z_1$  and  $z_2$  are always parallel to each other (see Fig. 2.12b). The transformation matrix of link 3 with respect to link 1 can be written as

$$\mathbf{Q}_1 = \mathbf{R}_{(z_1, \theta_1)} \mathbf{R}_{(y_1, \theta_2)} \mathbf{R}_{(y_2, -\theta_2)} \mathbf{R}_{(z_2, \theta_3)} = \mathbf{R}_{(z_1, \theta_1)} \mathbf{R}_{(z_2, \theta_3)} \quad (2.27)$$

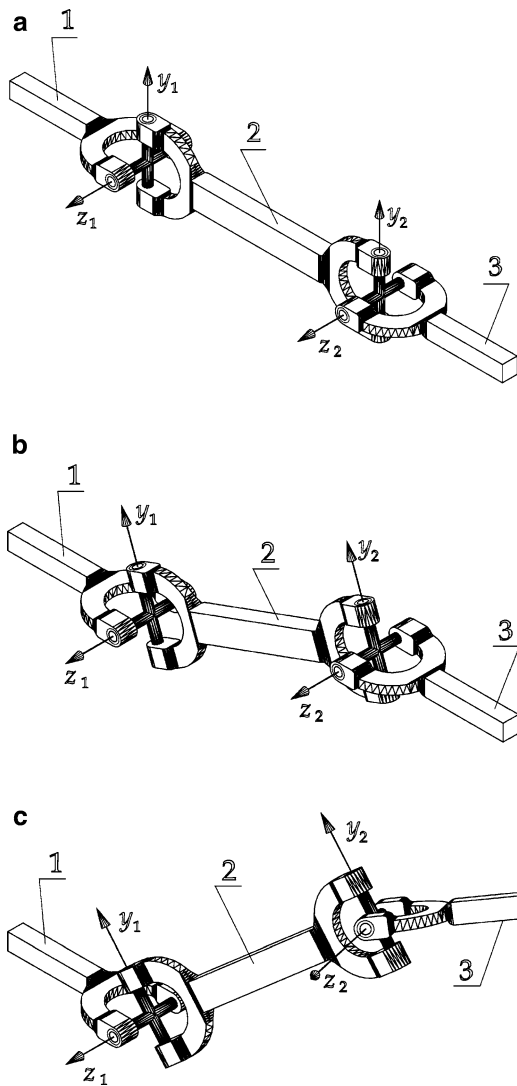
where  $\mathbf{R}_{(z_1, \theta_1)}$  stands for the transformation matrix when it rotates at angle  $\theta_1$  about the  $z_1$ -axis. The other matrices follow this rule. Equation (2.27) indicates that link 3 applies no self-rotation during translational motion.

When the movement of link 3 is of spatial type with respect to link 1 (Fig. 2.12c), the transformation matrix of link 3 with respect to link 1 is

$$\mathbf{Q}_2 = \mathbf{R}_{(z_1, \theta_1)} \mathbf{R}_{(y_1, \theta_2)} \mathbf{R}_{(y_2, \theta_3)} \mathbf{R}_{(z_2, \theta_4)} \quad (2.28)$$



**Fig. 2.12** Kinematic characteristic analysis of a UU chain: **(a)** initial configuration, **(b)** configuration when links 1 and 3 are parallel to each other, and **(c)** configuration when links 1 and 3 are not parallel to each other

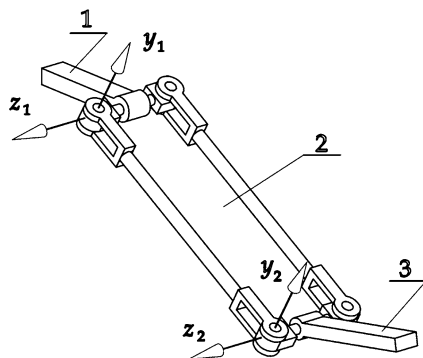


Given that the  $y_1$ -axis is always parallel to the  $y_2$ -axis, Eq. (2.28) can be rewritten as

$$\mathbf{Q}'_2 = \mathbf{R}_{(z_1, \theta_1)} \mathbf{R}_{(y', \theta_2 + \theta_3)} \mathbf{R}_{(z_2, \theta_4)} \quad (2.29)$$

which is actually the transformation matrix with Euler-angle  $z$ - $y$ - $z$  convention. Therefore, when the UU chain changes its initial configuration to the configuration that links 1 and 3, and these links are not parallel to each other, link 3 has three rotations with respect to link 1, including a self-rotation.

**Fig. 2.13** Substitute of the UU chain



Thus, we draw the following conclusions: (a) When the UU chain is at its initial configuration, it can constrain the self-rotation of link 3. (b) When the movement of link 3 is translational with respect to link 1, link 3 does not apply self-rotation. (c) If the movement of link 3 is spatial with respect to link 1, the self-motion of link 3 occurs.

The analysis above shows that the PUU chain in the mechanism of Fig. 2.11 cannot completely constrain the rotation of the mobile platform about the  $x$ -axis, indicating that the parallel mechanism has four DOFs at certain configurations. Figure 2.12 and Eq. (2.28) show that to constrain the rotation, the two inner revolute joints of the UU chain should be parallel to each other; the same applies to the two outer revolute joints. Only in this geometric condition can the mechanism shown in Fig. 2.11 have three spatial DOFs, i.e., two translations and one rotation.

In practice, however, the geometric condition cannot be satisfied at any moment. *Is there any substitute mechanism for the UU chain?*

To solve the problem of the UU chain, we provide a solution (Fig. 2.13), in which the UU combination is replaced by a revolute joint, planar parallelogram, and another revolute joint. The axes of the two revolute joints are parallel to each other and are orthogonal to those of the four revolute joints in the parallelogram. This arrangement guarantees constant parallelism between axes  $y_1$  and  $y_2$  and axes  $z_1$  and  $z_2$ . The solution is called the variation of the UU chain, referred to as the R(Pa)R chain. With this variation, when link 3 moves with respect to link 1, self-rotation no longer occurs.

The PUU chain in the mechanism in Fig. 2.11 can be replaced by the PR(Pa)R chain shown in Fig. 2.14. The new parallel mechanism (Liu et al. 2001a) is illustrated in Fig. 2.15. It has three DOFs, which are the translations in the  $O$ - $yz$  plane and the rotation about the line passing through the two S joints attached to the mobile platform.

### 2.3.1.2 Concept of a Parallelogram

*Why can a parallelogram solve the problem of the UU chain?* The concept of the parallelogram was used in some other parallel mechanisms. In the DELTA

**Fig. 2.14** Variation of the PUU chain, a PR(Pa)R chain

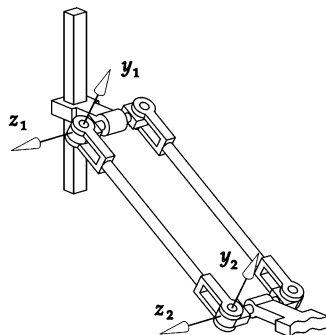
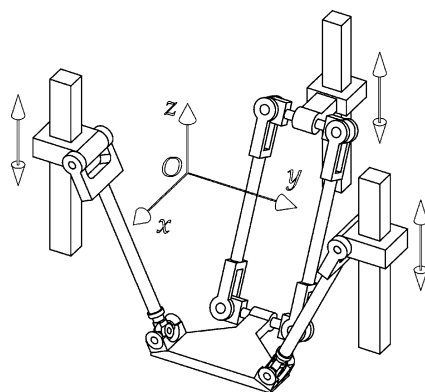


**Fig. 2.15** Spatial 3-DOF parallel mechanism with a 2-PRS&1-PR(Pa)R chain (Liu et al. 2001a)

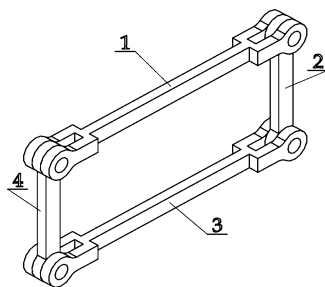


mechanism (Fig. 1.22), each of the three legs consists of a spatial four-bar mechanism. The four bars are connected end to end by spherical joints. Although it is a spatial mechanism, each two of the four bars should be parallel to each other at every instant, for which DELTA has three translational DOFs. The design concept was extended to a new family of 4-DOF parallel mechanisms, H4 (Fig. 1.32), in 1999. Such a concept is highly important to parallel mechanism design in which a planar four-bar parallelogram is used.

The mechanism of the planar four-bar parallelogram lies in four bars connected end to end by revolute joints. Figure 2.16 shows that links 1 and 3, as well as links 2 and 4, are identical in link length. Links 1 and 2 can always have identical orientations with links 3 and 4, respectively. The parallelogram was first applied to the design of the StarLike mechanism (Fig. 1.24) in 1992 by Hervé; this mechanism also has three translational DOFs, used later in the design of another parallel mechanism (Fig. 1.23) with three translational DOFs by Tsai in 1996. From then on, the concept of the parallelogram has attracted the attention of many researchers. Application examples include TURIN (Sorli et al. 1997) with six DOFs and CaPaMan (Ceccarelli 1997) with three DOFs.

Although the locus of any point on the output link is a circle, a planar parallelogram enables an output link to maintain a fixed orientation with respect to

**Fig. 2.16** Planar parallelogram



an input link, which is why the concept of the parallelogram is used in these parallel manipulators. In particular, addressing the UU chain (as shown in Sect. 4.1.1) is highly useful. In the above-mentioned designs, the parallelogram guarantees desired output, such as no rotational DOFs for StarLike and Tsai's mechanisms.

Conversely, the planar parallelogram, being a leg, can improve the kinematic performance of a system. Typically, the constant link in a leg for most parallel mechanisms is only a single bar. If the leg is constructed by a simple mechanism, a parallel mechanism will have better performance in terms of kinematics and dynamics. The first design that employed a simple mechanism in leg kinematics is a micromotion mechanism proposed by Hudgens and Tesar (1988). In this mechanism, each leg is driven by a four-bar mechanism mounted on the base, an approach that improved the positional resolution of the mechanism. Tahmasebi (1992) presented a 6-DOF parallel mechanism by means of the planar 2-DOF five-bar mechanism; the positional resolution, stiffness, and force control of the mechanism were improved. Frisoli et al. (1999) developed a novel tendon-driven five-bar linkage with a large isotropic workspace and applied it to the legs of a 6-DOF haptic device, thereby generating good kinematic isotropy and acceleration. Moreover, Chung and Lee (2001) proposed a new 2-DOF parallel mechanism, in which each leg includes a four-bar mechanism, showing advantages in terms of good kinematic performance and static balance (Wang and Gosselin 1999).

Another advantage to designing a mechanism with a parallelogram acting as the constant link in each leg is that leg stiffness can be increased to a large extent. A parallelogram has higher stiffness with respect to a single bar. Moreover, leg stiffness can be improved further by increasing redundant constraints. For instance, the parallelogram can be designed as in Fig. 2.17, in which the number of parallelograms is increased. The more parallelograms the leg has, the higher the stiffness of the mechanism and, relatively, the higher the fabrication accuracy required because of the redundant constraints.

For most parallel mechanisms, rotational capability reaches its maximum at the original point of the workspace. The maximum value is usually limited for some parallel mechanisms with spherical joints because of the limited swing angle of such joints. Moreover, the tilting angle of the mobile platform becomes increasingly smaller from the point to the boundary. A parallelogram enables the output link to remain at a fixed orientation with respect to an input link in such a way that attaching

**Fig. 2.17** Parallelogram with redundant constraints

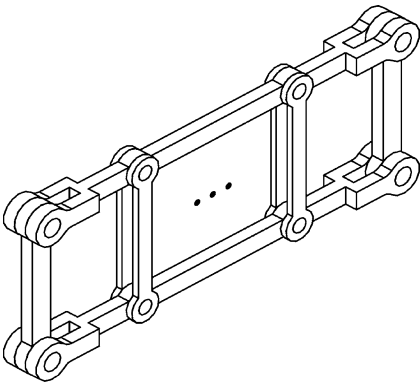
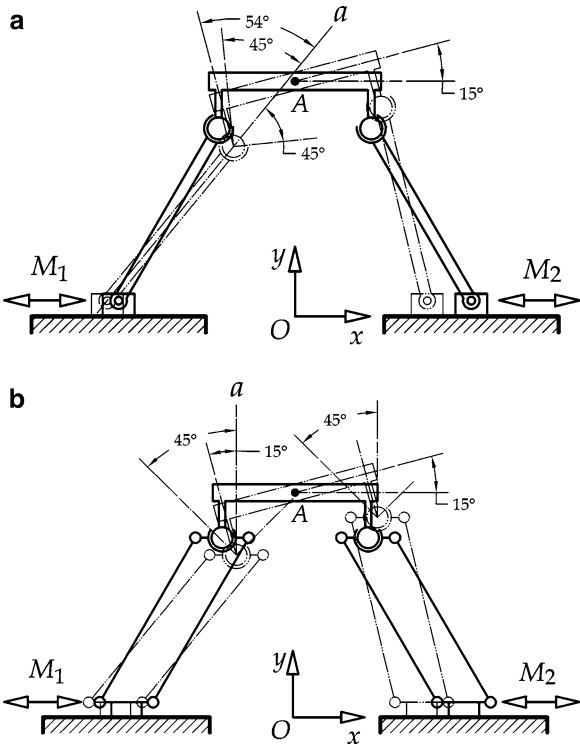


**Fig. 2.18** Rotational capability comparison of two kinds of leg mechanisms: (a) with a single bar and (b) with a planar four-bar parallelogram



one end of a ball-and-socket joint to the output link can relatively increase the swing range of the joint. The method eventually improves the rotational capability of the mobile platform. For example (refer to Fig. 2.18), suppose that in some kind of parallel mechanism, the combination of actuations  $M_1$  and  $M_2$  enables the mobile platform to rotate about point A. In Fig. 2.18a, each of the two legs is a traditional one, which consists of a length-fixed link. The link is connected to the mobile

platform by a ball-and-socket joint. In Fig. 2.18b, each leg consists of a planar four-bar parallelogram, which is also connected to the mobile platform by a ball-and-socket joint. The socket is fixed to the output link of each parallelogram. In Fig. 2.18, line  $a$  is the reference line, from which the tilting angle for the joints is limited to  $\pm 45^\circ$ . Let each mobile platform rotate  $15^\circ$  about original point  $A$  from zero orientation. Figure 2.16 shows that the orientation of line  $a$  in Fig. 2.18a is variable according to the change in the orientation of the link but maintains invariable in Fig. 2.16b. For this reason, the ball-and-socket joint in Fig. 2.16a exceeds the tilting limit at the  $15^\circ$  orientation because of  $54.2^\circ > 45^\circ$ . In Fig. 2.16b, however, the joint has not reached its limit. Therefore, the mobile platform in Fig. 2.16b can yield higher rotational capability than can that in Fig. 2.16a, for which we can conclude that a parallel mechanism with a parallelogram in its leg may obtain higher rotational capability than can the traditional one. Moreover, because the socket maintains its original orientation at every instant, the rotational capability at the point near the original point does not diminish.

The advantages of using parallelograms in the design of parallel mechanism are clear: desired DOF output, considerably higher stiffness, higher rotational capability, and good kinematic and dynamic performance. The disadvantage stems from the complex structure when evaluated against the combination of a revolute joint and one constant link. A parallelogram has four revolute joints and four links. The axes of all the joints should be parallel to one another, and the lengths of each two of the four links should be equal to one another as well. Therefore, the fabrication accuracy should be sufficiently high enough; otherwise, accumulation of errors occurs, eventually resulting in error accumulation in the device. All the joints have single DOFs, but this is not a critical problem. Considering the advantages that the parallelogram offers, the complex structure is acceptable.

Maximizing the advantage of the desired output of a planar four-bar parallelogram, some researchers proposed parallel mechanisms (Liu and Wang 2003, 2005; Liu et al. 2005b).

### 2.3.1.3 Some Parallel Mechanisms Containing a Planar Parallelogram

Some parallel mechanisms can be designed on the basis of the concept of a parallelogram. In these designs, a parallelogram plays a key role in desired DOF output as well as in improved rotational capability and stiffness.

#### Two-DOF Parallel Mechanisms

The most planar 2-DOF parallel mechanisms (Figs. 3.1 and 3.2) are the five-bar mechanisms with prismatic or revolute actuators. The mechanism with revolute actuators comprises five revolute pairs, and the two joints fixed to the base are actuated (Fig. 3.1f). The output of the mechanism is the translational motion of a point on the end-effector. Figure 3.1f shows that the locus of any point on the

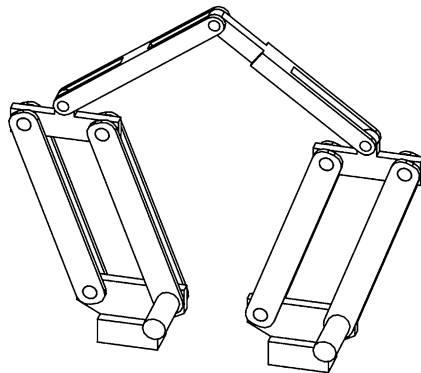


**Fig. 2.19** Two-DOF parallel mechanism with a (Pa)RRR(Pa) chain

proximal link, i.e., the actuated link, is a circle, which is the same as that of a point on the output link of a parallelogram. This feature reminds us to replace the proximal link with a parallelogram. The new parallel mechanism is shown in Fig. 2.19. In the same manner, the RRRPR and RRRRP mechanisms shown in Fig. 1.12b and e can be replaced by (Pa)RRPR and (Pa)RRRP, respectively. Figure 2.20a shows another planar 2-DOF parallel mechanism with a (Pa)RR(Pa)P chain, in which one revolute joint in the first (Pa) and the prismatic joint are active. The mobile platform also has two planar DOFs. In these designs, the parallelogram is a substitute for the combination of a revolute joint and a length-fixed link in each leg. This substitution improves the stiffness of the leg. The design shown in Fig. 2.20b differs from those in Figs. 2.19 and 2.20a. It consists of two R(Pa)R chains. In this design, if revolute actuator  $M_1$  is locked, the mechanism is equivalent to a planar four-bar mechanism with actuator  $M_2$ . If  $M_1$  is active but  $M_2$  is locked, the mechanism undergoes translation along the  $x$ -axis. At the same time, rotation about the  $x$ -axis occurs; this rotation is an associated movement. Thus, the output is the translation along the  $x$ -axis and another translation in the  $O$ - $yz$  plane or a rotation about the  $x$ -axis.

As previously mentioned, the output of most planar 2-DOF parallel mechanisms is the planar motion of a point, while orientation changes instantly. In some applications, an object should be transferred with fixed orientation. In such a case, the translational motion of a rigid body with fixed orientation is needed, and the above-mentioned 2-DOF parallel mechanisms are unavailable. The design based on a parallelogram can be used to address this problem. Such a parallel mechanism with a 2-P(Pa) chain is shown in Fig. 2.21a; the two translational DOFs can be achieved if the prismatic joints are active. To obtain the two DOFs of a rigid body in this system, the P(Pa)&PRR kinematic chain shown in Fig. 2.21b is sufficient for guaranteeing the mechanism with two translational DOFs. Two planar four-bar parallelograms are used to increase the stiffness of the system and make the system symmetrical. The parallel mechanism has been applied to the development

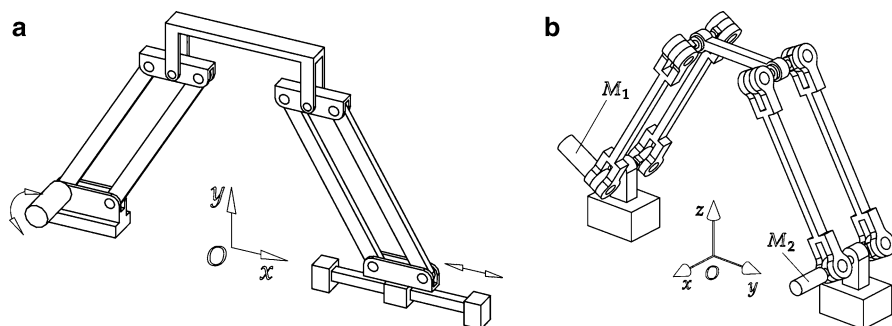


**Fig. 2.20** Two kinds of planar 2-DOF parallel mechanisms: (a) with a (Pa)RR(Pa)P chain and (b) with a 2-R(Pa)R chain

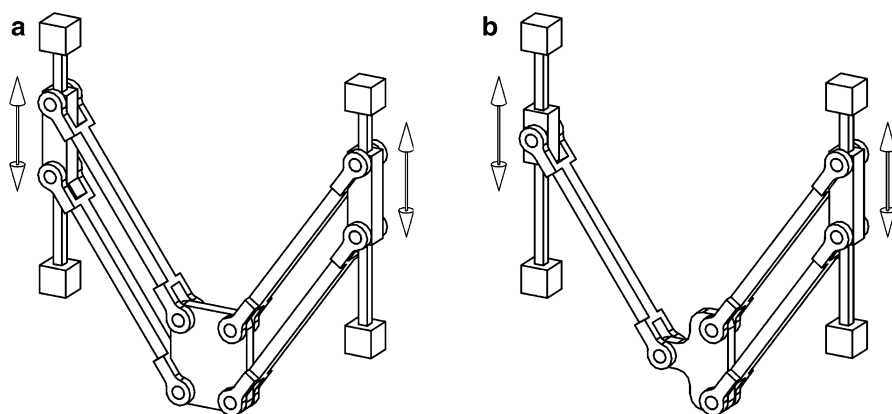


**Fig. 2.21** Parallel mechanisms with two pure translational DOFs: (a) with symmetrical architecture and (b) with asymmetrical architecture

of a five-axis hybrid machine tool (Liu 2001; Liu et al. 2005c), which is now being used to machine a kind of impeller. In the mechanisms shown in Fig. 2.21, some P joints can be replaced by four-bar planar parallelograms. For example, the parallel mechanisms can be equipped with the 4(Pa) and 2(Pa)&3R chains. The latter is illustrated in Fig. 2.22.

Some two-DOF parallel mechanisms based on the above-mentioned design concept are listed in Table 2.1.

The output link of a planar parallelogram has one DOF, and its orientation remains constant. The output link of a double-parallelogram mechanism, denoted as the (Pa)(Pa) chain, should have two DOFs, and its orientation is also constant. Therefore, we can design a 2-DOF parallel mechanism that consists of three legs, with the third one being a passive (Pa)(Pa) chain and the two others active. Each of the actuated legs can be a 3-, 4-, 5- or 6-DOF chain. At the least, it must be a 3-DOF chain, as in the PRR, RRR, RPR, or PPR chain. As an example, the parallel



**Fig. 2.22** Two-DOF translational parallel mechanism with a 2(Pa)&3R chain

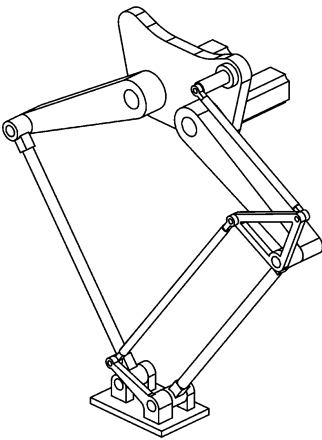


**Table 2.1** Some 2-DOF parallel mechanisms

No.	Leg chains		Mechanism chains	Remarks
	First leg	Second leg		
1	(Pa)RR	(Pa)RR	(Pa)RRR(Pa)	As shown in Fig. 2.17
2	(Pa)RR	RPR	(Pa)RRPR	Comes from the RRRPR mechanism
3	(Pa)RR	PRR	(Pa)RRRP	Comes from the RRRRP mechanism
4	(Pa)R	P(Pa)R	(Pa)R&P(Pa)R	Fig. 2.18a
5	R(Pa)R	R(Pa)R	2-R(Pa)R	Fig. 2.18b
6	P(Pa)	P(Pa) or PRR	P(Pa)(Pa)P(or P(Pa)PRR)	There are two cases: the actuated P joint can be vertical or horizontal. The vertical case is shown in Fig. 2.19
7	(Pa)(Pa)	(Pa)(Pa) or RRR	4(Pa) (or 2(Pa)&3R)	In each leg, a revolute joint in the input link of the parallelogram that attached to the base is actuated. The 2(Pa)&3R mechanism is shown in Fig. 2.20

mechanisms with 2-PRR&1-(Pa)(Pa) and 2-RPR&1-(Pa)(Pa) chains are shown in Fig. 2.23a, b, respectively. Because of the double-parallelogram mechanism, both mechanisms have two pure translational DOFs. A prismatic joint cannot change the slider orientation; thus, the double-parallelogram chain can be replaced by a prismatic parallelogram, referred to as the P(Pa) chain, shown in Fig. 2.24. The possible 2-DOF translational parallel mechanisms with a passive leg are listed in Table 2.2, and a typical instance is illustrated in Fig. 2.25.

Three-DOF Parallel Mechanisms

As introduced in Sect. 3.1.2, many kinds of parallel mechanisms with three DOFs are available. An example is the planar 3-RRR parallel mechanism (Fig. 1.15). The mobile platform has three planar DOFs, which are two translations in the *O-xy* plane

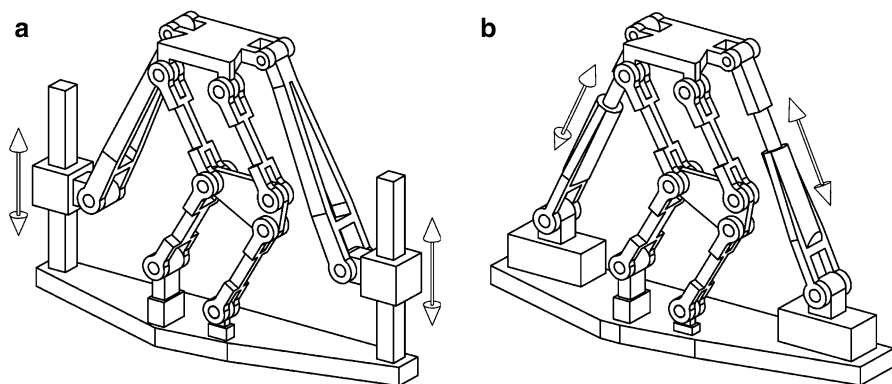


**Fig. 2.23** Two 2-DOF translational parallel mechanisms: (a) with two active PRR chains and one passive (Pa)(Pa) chain and (b) with two active RPR chains and one passive (Pa)(Pa) chain

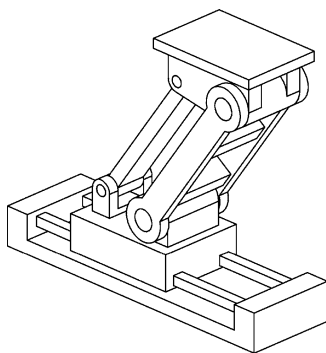


**Fig. 2.24** P(Pa) kinematic chain

and a rotation around the Z-axis. To increase the stiffness of each leg, a 3-DOF parallel mechanism with parallelograms is employed (Fig. 2.26). This mechanism is kinematically equivalent to the architecture in Fig. 1.15. Similarly, two types of such mechanisms with 3-P(Pa)R chains, which are equivalent to those with 3-PRR chains, are shown in Fig. 2.27. Figure 2.28 shows four types of spatial 3-DOF 3-[PP]S parallel mechanisms, which are the modified versions of the 3-RPS and 3-PRS parallel mechanisms. Comparatively, they possess higher rotational capability and stiffness. In the mechanism shown in Fig. 2.28a, either the P joint or one R joint of the parallelogram attached to the base in each leg can be active. In the three others, the P joints are actuated.

Figure 2.29 shows another spatial 3-DOF parallel mechanism with a 1-R(Pa)R&2-RR(Pa)R chain. If actuator  $M_1$  is locked, the mechanism is equivalent to a planar 2-DOF mechanism with actuators  $M_2$  and  $M_3$ . Thus, the output is the translation along the z-axis and two planar motions in the  $O$ -xy plane. Its kinematic chain can also be 1-R(Pa)R&2-PR(Pa)R.

**Table 2.2** Some 2-DOF translational parallel mechanisms with a passive leg

No.	Leg chains		Mechanism chains	Remarks
	First and second legs	Passive leg		
1	RRR	(Pa) (Pa) or P(Pa)	2-RRR&1-(Pa)(Pa) or 2-RRR&1-P(Pa)	
2	PRR		2-PRR&1-(Pa)(Pa) or 2-PRR&1-P(Pa)	The 2-PRR&1-(Pa)(Pa) mechanism is shown in Fig. 2.23a
3	RPR		2-RPR&1-(Pa)(Pa) or 2-RPR&1-P(Pa)	
4	RRU		2-RRU&1-(Pa)(Pa) or 2-RRU&1-P(Pa)	
5	PRU		2-PRU&1-(Pa)(Pa) or 2-PRU&1-P(Pa)	
6	RPU		2-RPU&1-(Pa)(Pa) or 2-RPU&1-P(Pa)	
7	RRS		2-RRS&1-(Pa)(Pa) or 2-RRS&1-P(Pa)	
8	PRS		2-PRS&1-(Pa)(Pa) or 2-PRS&1-P(Pa)	The 2-PRS&1-P(Pa) mechanism is shown in Fig. 2.25
9	RPS		2-RPS&1-(Pa)(Pa) or 2-RPS&1-P(Pa)	
10	UPS		2-UPS&1-(Pa)(Pa) or 2-UPS&1-P(Pa)	
11	PUS		2-PUS&1-(Pa)(Pa) or 2-PUS&1-P(Pa)	
12	URS		2-URS&1-(Pa)(Pa) or 2-URS&1-P(Pa)	
13	RUS		2-RUS&1-(Pa)(Pa) or 2-RUS&1-P(Pa)	

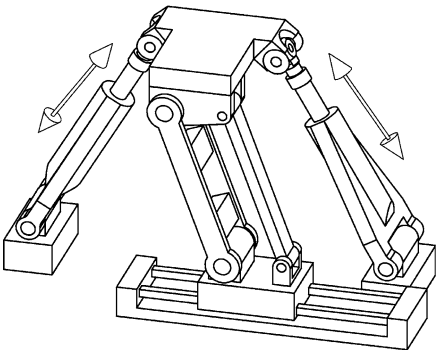


**Fig. 2.25** Two-DOF translational parallel mechanism with a 2-PRS&1-P(Pa) chain

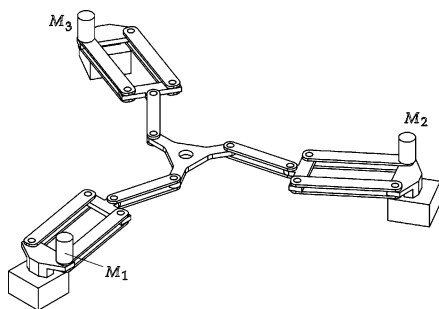


**Fig. 2.26** Planar 3-(Pa)RR parallel mechanism

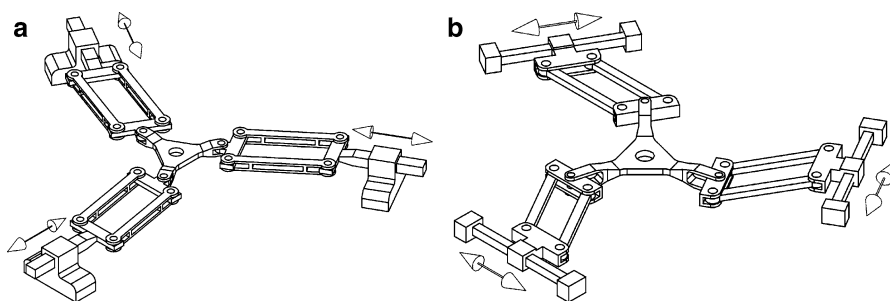


**Fig. 2.27** Two kinds of planar 3-P(Pa)R parallel mechanisms

To solve the problem of the UU chain, an R(Pa)R chain was proposed (Fig. 2.11). Accordingly, the 2-PRS&1-PUU mechanism was revised as the 2-PRS&1-PR(Pa)R mechanism (see Fig. 2.15). The observation of the revised mechanism shows that because the PR(Pa)R chain constrains two rotations, a redundant DOF exists in the two spherical joints. Thus, the two PRS chains can be replaced by two PRU chains. The modified mechanism is shown in Fig. 2.30. The topological mechanism with revolute actuators is illustrated in Fig. 2.31. In the two mechanisms, the first and second legs should be in the same plane. Moreover, in these two legs, two axes for the revolute joints in the U joints that are connected to the mobile platform should be collinear. The axis of the revolute joint in the third leg linked to the mobile platform should be parallel to these two axes. Therefore, the two mechanisms have two translations in the  $O$ -yz plane and one rotation about the collinear line. The mechanisms shown in Figs. 2.15 and 2.30 have very high rotational capability and are analyzed in the subsequent chapters.

The collinear axes for the two revolute joints of the mechanism in Fig. 2.30 motivate the redesign of the first and second legs (Fig. 2.32). In these two designs, the two revolute joints are combined into one revolute joint. Figure 2.32a shows that the first and second legs are connected to the mobile platform through one

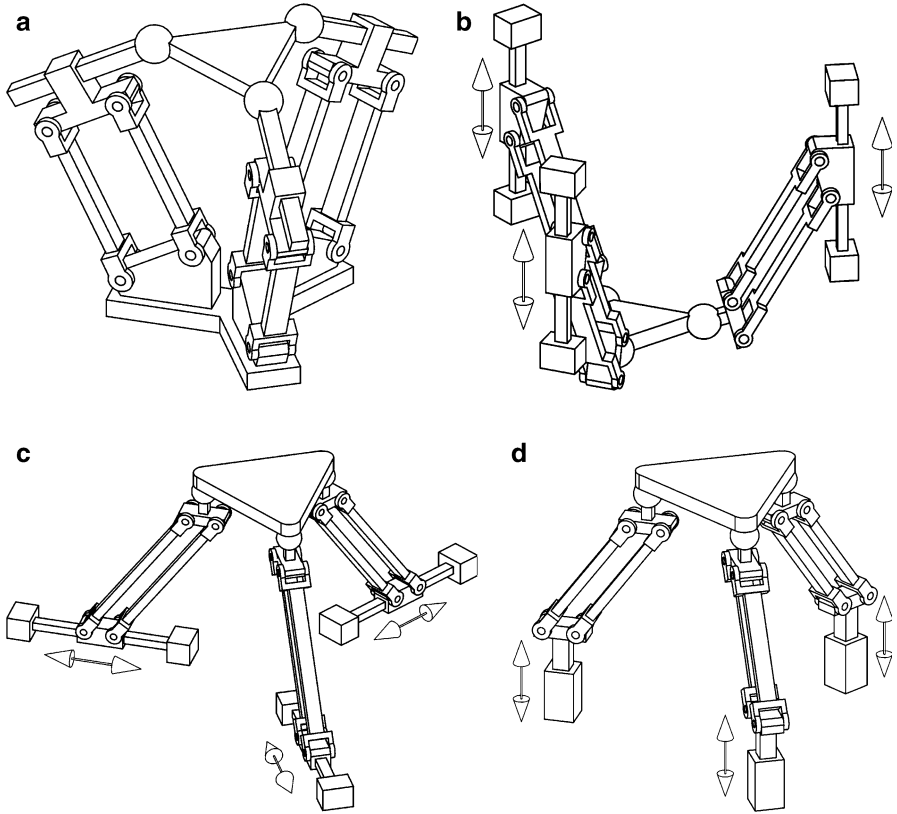


Fig. 2.28 Four kinds of 3-[PP]S parallel mechanisms

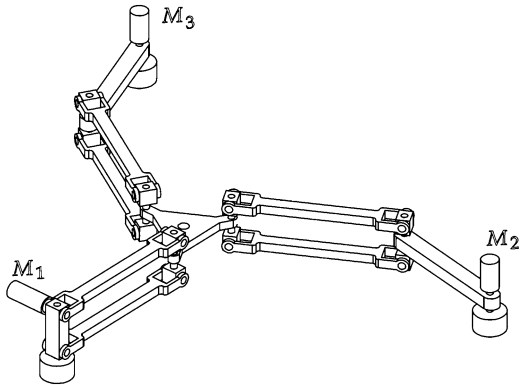
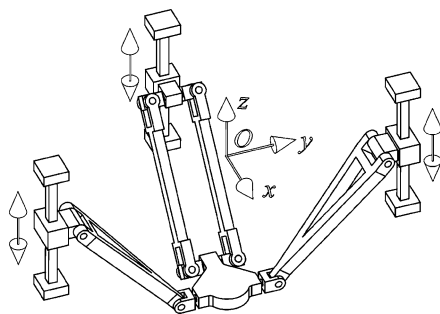
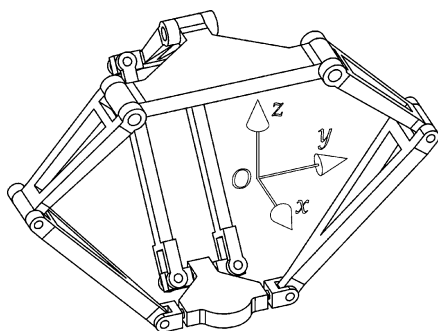


Fig. 2.29 Spatial 3-DOF parallel mechanism with 1-R(Pa)R&2-RR(Pa)R



**Fig. 2.30** Three-DOF parallel mechanism with a 2- $\underline{\text{PRU}}$ &1- $\underline{\text{PR(Pa)R}}$  chain



**Fig. 2.31** Three-DOF parallel mechanism with a 2- $\underline{\text{RRU}}$ &1- $\underline{\text{RR(Pa)R}}$  chain

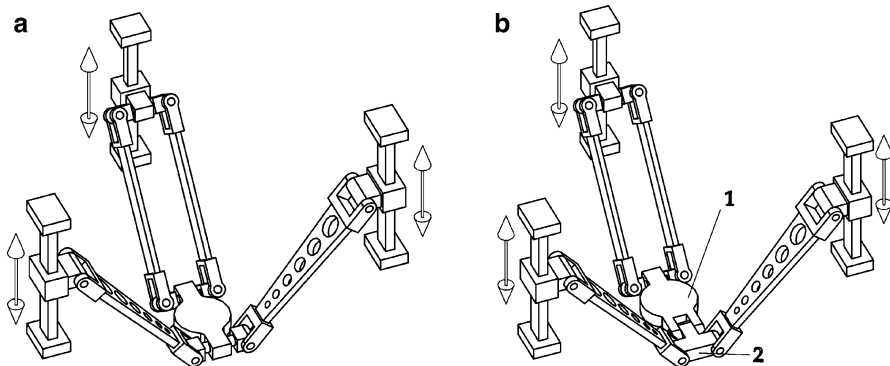


**Fig. 2.32** Two topological mechanisms of the mechanism shown in Fig. 2.30

revolute joint. As shown in Fig. 2.32b, the first and second legs with PRR chains are connected to a constant orientation bar 2, which is linked to mobile platform 1 by a revolute joint. If the kinematic chain for the mechanism shown in Fig. 2.30 is 2- $\underline{\text{PRU}}$ &1- $\underline{\text{PR(Pa)R}}$ , the chain for the two designs will be  $(\text{PRR})_2\text{R}\&\underline{\text{PR(Pa)R}}$ .

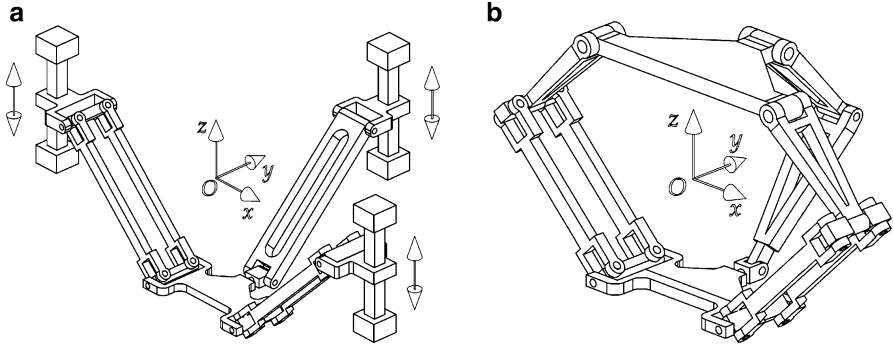


**Fig. 2.33** Two spatial 3-DOF parallel mechanisms: **(a)** with a 2-PR(Pa)R&1-PRU chain and **(b)** with a 2-RR(Pa)R&1-RRU chain

**Table 2.3** Constraint and DOFs of the parallel mechanism in Fig. 2.33a

Single leg			Combination of three legs	
No.	Chain type	Constraints	Constraints	Remained DOFs
1	PR(Pa)R	$\{RO_x, RO_z\}$	$\{T_x, RO_x, RO_z\}$	$\{T_y, T_z, RO_y\}$
2	PR(Pa)R	$\{RO_x, RO_z\}$		
3	PRU	$\{T_x, RO_z\}$		

This modification, which has no negative influence on the rotational capability of the mechanism, can also be extended to the mechanism (Fig. 2.31) with revolute actuators.

The kinematic chains in the mechanism in Fig. 2.30 shows that the end-effector of a PR(Pa)R chain has three translations and one rotation, and that of a PRU chain has two translations and two rotations. A mechanism with two PRU chains and one PR(Pa)R chain has two translational DOFs and one rotational DOF. *What about a mechanism with two PR(Pa)R chains and one PRU chain?* Such a mechanism (Liu et al. 2005a) is shown in Fig. 2.33a, in which the three R joints attached to the mobile platform are parallel with the others. When the three P joints are active, the mechanism should have three DOFs. The mechanism with revolute actuators is shown in Fig. 2.33b. Given the arrangement of links and joints of the mechanism, the combination of the three legs constrains the rotation of the mobile platform with respect to the  $x$ - and  $z$ -axes as well as with the translation along the  $x$ -axis. This leaves the two mechanisms with two translational DOFs in the  $O$ - $yz$  plane and one rotational DOF about the  $y$ -axis. Table 2.3 shows the capability description of the mechanism with prismatic actuators. The mechanisms shown in Figs. 2.30 and 2.33a have the same output, but there is an outstanding difference between them in terms of the rotational DOF: the latter is actuation redundant for the DOF but the former is not. That is, the rotational DOF of the latter is determined by the combination of the first and second legs with PR(Pa)R chains. This situation is similar to the mechanisms shown in Figs. 2.31 and 2.33b.

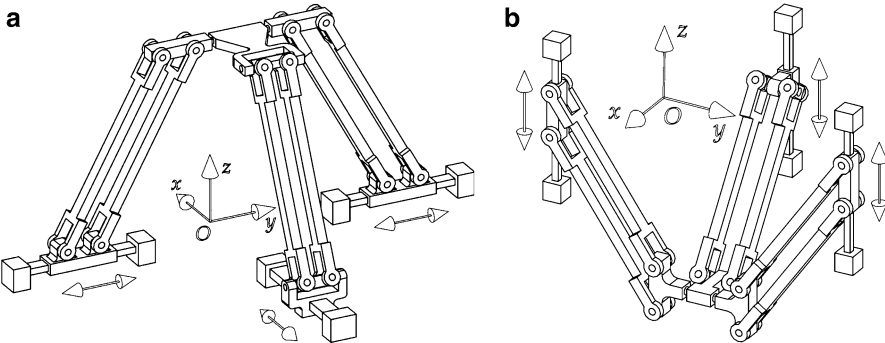


**Fig. 2.34** Kinematic architecture of the parallel mechanism with a 2-P(Pa)R&1-PR(Pa)R chain

**Table 2.4** Constraint and DOFs of the parallel mechanism in Fig. 2.34

Single leg			Combination of three legs	
No.	Chain type	Constraints	Constraints	Remained DOFs
1	P(Pa)R	$\{RO_x, RO_z, T_x\}$	$\{T_x, RO_x, RO_z\}$	$\{T_y, T_z, RO_y\}$
2	P (Pa)R	$\{RO_x, RO_z, T_x\}$		
3	PR(Pa)R	$\{RO_x, RO_z\}$		

Let us consider another spatial 3-DOF parallel mechanism (Fig. 2.34). The mechanism has two P(Pa)R chains and one PR(Pa)R chain. Table 2.4 presents the capability of the mechanism in detail, showing that the first leg itself can constrain the mobile platform with the translation along the  $x$ -axis and rotations about the  $z$ - and  $x$ -axes. The second leg can be identical to or different from the first leg (e.g., the second leg can be equipped with a PRU chain). The combination of the first and second legs can also impose the same constraints on the mechanism, i.e., the translation along the  $x$ -axis and rotations about the  $z$ - and  $x$ -axes. Moreover, the third leg can be a 4-, 5-, or 6-DOF chain (e.g., a PUU or PUS). It can also be a traditional PSS chain. The possible chains for the three legs and mechanism are shown in Table 2.5. The table demonstrates that six types of mechanisms have different legs. For example, the mechanisms with P(Pa)R-PRU-PR(Pa)R and P(Pa)R-P(Pa)R-PUU chains are shown in Fig. 2.35a, b, respectively. In the PUU chain, the axis of the revolute joint in the first U joint that is attached to the P joint and the axis of the revolute joint in the second U joint that is connected to the mobile platform must both be parallel to the  $y$ -axis. Then, the mechanisms can also have three DOFs, which are two translational DOFs in the  $O$ - $yz$  plane and one rotational DOF about the  $y$ -axis. For the PUS chain in Table 2.5, the axis of the revolute joint in the first U joint that is attached to the P joint should also be parallel to the  $y$ -axis. Many topological architectures based on such a concept have been proposed, but these are not comprehensively described in this chapter.

We compare the mechanism shown in Fig. 2.34 and its topological mechanisms with the mechanism in Fig. 2.30. They have the same output, but there are some



**Table 2.5** Possible legs and topological mechanisms of the parallel mechanism in Fig. 2.34

Leg chain			Mechanism chains
First leg	Second leg	Third leg	
P(Pa)R	P(Pa)R	PR(Pa)R	P(Pa)R-P(Pa)R-PR(Pa)R
			P(Pa)R-PRU-PR(Pa)R
	PRU	PUU	P(Pa)R-P(Pa)R-PUU
			P(Pa)R-PRU-PUU
		PUS (or PSS)	P(Pa)R-P(Pa)R-PUS
			P(Pa)R-PRU-PUS

Where *P* prismatic joint, *R* revolute joint, *U* universal joint, (*Pa*) parallelogram, *S* spherical joint

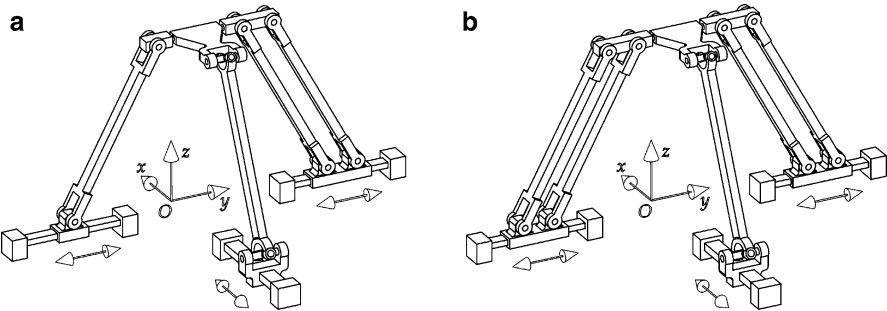


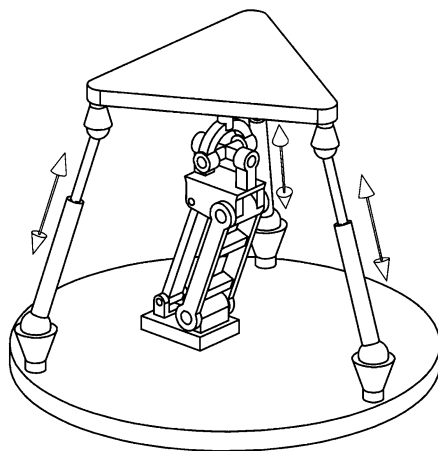
**Fig. 2.35** Two kinds of topological architectures of the mechanism in Fig. 2.34a

differences between them. In the mechanism in Fig. 2.30, the first and second legs are PRU chains, which can constrain the mobile platform with the translation along the *x*-axis and the rotation about the *z*-axis. The combination of the two legs causes the mobile platform to rotate freely about the line parallel to the *x*-axis. Because it is the undesirable output, the rotational DOF should be constrained by the third leg. In such a situation, the stiffness of the third leg should be sufficiently high for addressing the inner torque of the mobile platform. Conversely, in the mechanism shown in Fig. 2.34, the first and second legs themselves can constrain the rotation about the *x*-axis; no additional requirement on the stiffness of the third leg is necessary. As a result, the system stiffness of the mechanism is relatively higher.

Similar to a 2-DOF parallel mechanism, the planar four-bar parallelogram can also be used in the design of a 3-DOF parallel mechanism with a passive leg. As an example, Fig. 2.36 shows a spatial 3-DOF parallel mechanism with three active UPS chains and one passive leg with a (Pa)U chain, which leads to one degree of translational freedom and two degrees of rotational freedom of the mechanism.

The possible 3-DOF parallel mechanisms with a planar four-bar parallelogram are listed in Table 2.6.

**Fig. 2.36** Spatial 3-DOF parallel mechanism with a passive leg



#### Four-DOF Parallel Mechanisms

Several parallel mechanisms with four DOFs can be designed on the basis of the concept of a four-bar parallelogram. Figure 2.37a shows a 4-DOF parallel mechanism with a 2-PR(Pa)U & 2-PR(Pa)R chain, and in Fig. 2.37b, the mechanism is equipped with a 2-PUU & 2-PR(Pa)R chain. The mobile platforms for both these mechanisms have four DOFs, which are three translations and one rotation about the  $y$ -axis with respect to the base. If the quadrangle of the mobile platform is similar to that of the base, the mechanisms will be in their singular configurations at the original position.

Figure 2.38 shows two kinds of 4-DOF parallel mechanisms with a passive leg. Each of these designs is equipped with four legs having UPS (or SPS) chains, in which the P joint is actuated; the fifth (passive) leg in the mechanism in Fig. 2.38a has a (Pa)PU chain; and the mechanism in Fig. 2.38b has a (Pa)S chain.

The other parallel mechanisms with four DOFs are listed in Table 2.7.

#### Five-DOF Parallel Mechanisms

As mentioned earlier, designing a 5-DOF symmetrical parallel mechanism is difficult. Such a mechanism with fully symmetric architecture is also difficult to design using a parallelogram. Two kinds of 5-DOF parallel mechanisms with a parallelogram in one of their legs are illustrated in Fig. 2.39. In these designs, the fifth leg is actuated and also serves as the leading leg, i.e., the output of the mechanism is dependent on the leg. The other four legs are equipped with UPS or SPS chains, in which the P joints are also actuated. In Fig. 2.39a, the kinematic chain of the fifth leg is the P(Pa)S, and that in Fig. 2.39b is the P(Pa)PU, in which the prismatic joints attached to the base are actuated. Thus, the mechanisms have two translations and three rotations, as well as three translations and two rotations, respectively.

The other parallel mechanisms with five DOFs are enumerated in Table 2.8.

**Table 2.6** Some three-DOF parallel mechanisms with a planar four-bar parallelogram

Leg chains				Mechanism chains	Remarks
No.	First leg	Second leg	Third leg		
1	(Pa)RR	(Pa)RR	(Pa)RR	3-(Pa)RR	As shown in Fig. 2.26
2	P(Pa)R	P(Pa)R	P(Pa)R	3- P(Pa)R	Two examples are shown in Fig. 2.27
3	(Pa)PS	(Pa)PS	(Pa)PS	3- (Pa)PS	As shown in Fig. 2.28a
4	P(Pa)S	P(Pa)S	P(Pa)S	3- P(Pa)S	As shown in Fig. 2.28b-d
5	R(Pa)R	RR(Pa)R	RR(Pa)R	1-R(Pa)R&2-RR(Pa)R	As shown in Fig. 2.29
6	PRU(S)	PRU(S)	PR(Pa)R	2-PRU(S)&1-PR(Pa)R	As shown in Fig. 2.30
7	RRU(S)	RRU(S)	RR(Pa)R	2-RRU(S) & 1-RR(Pa)R	As shown in Fig. 2.31
8	PR(Pa)R	PR(Pa)R	PRU	2-PR(Pa)R&1-PRU	As shown in Fig. 2.33a
9	RR(Pa)R	RR(Pa)R	RRU	2-RR(Pa)R&1-RRU	As shown in Fig. 2.33b
10	P(Pa)R	P(Pa)R	PR(Pa)R	2-P(Pa)R&1-PR(Pa)R	Fig. 2.34, please see Table 2.5 for other topology architectures
The first, second and third legs					
11	UPS (PUS or RUS)	The fourth (passive) leg (Pa)U		3-UPS&1-(Pa)U	As shown in Fig. 2.36
12		(Pa)PR		3-UPS&1-(Pa)PR	
13		(Pa)RP		3-UPS&1-(Pa)RP	

Where  $P$  prismatic joint,  $R$  revolute joint,  $(Pz)$  parallelogram,  $S$  spherical joint

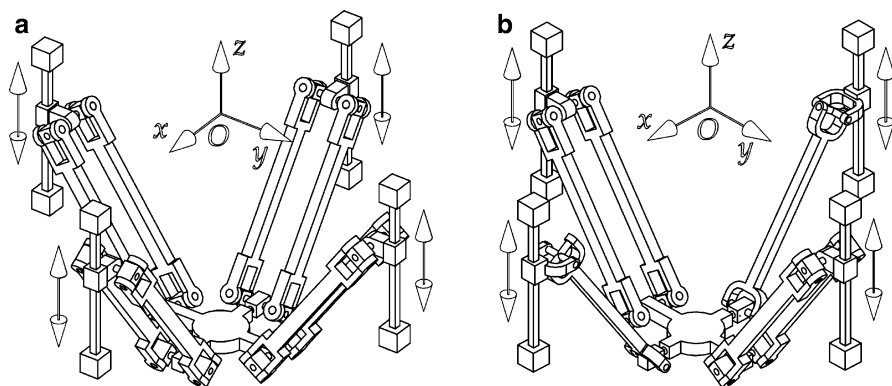


**Fig. 2.37** Two 4-DOF parallel mechanisms: (a) with a 2-PR(Pa)U & 2-PR(Pa)R chain and (b) with 2-PUU & 2-PR(Pa)R chain

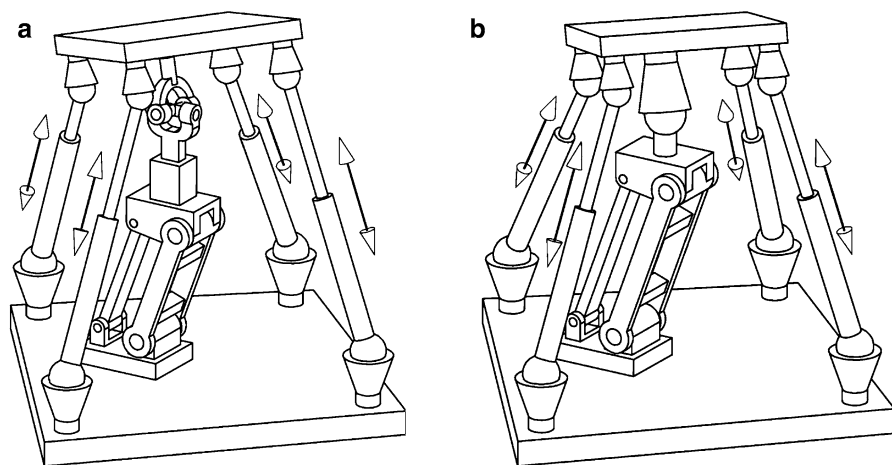


**Fig. 2.38** Two kinds of 4-DOF parallel mechanisms with a passive leg: (a) with a 4-SPS & 1-(Pa)PU chain and (b) with a 4-SPS & 1-(Pa)S chain

### Six-DOF Parallel Mechanisms

In the past two decades, 6-DOF parallel mechanisms have been the most frequently studied mechanisms. These mechanisms can provide all of the DOFs that a rigid body can have in 3-D space. This kind of parallel mechanism has been eliciting increasing attention in the field. Generally, each leg of this mechanism is a typical serial chain with six DOFs. The fully parallel mechanism is usually one that includes at least six such legs. Some 6-DOF parallel mechanisms have three legs. Two actuators are attached to each leg. Compared with a 6-DOF mechanism with six legs, a fully parallel mechanism has a considerably larger workspace, simpler forward and inverse kinematic solutions, and fewer moving parts and joints. The

**Table 2.7** Some four-DOF parallel mechanisms with a four-bar parallelogram

Leg chains				Mechanism chains	Remarks
No.	First leg	Second leg	Third leg Fourth leg		
1	PR(Pa)U	PR(Pa)R	PR(Pa)U PR(Pa)R	2-PR(Pa)U&2-PR(Pa)R	As shown in Fig. 2.37a
2	PUU	PR(Pa)R	PUU PR(Pa)R	2-PUU&2-PR(Pa)R	As shown in Fig. 2.37b
Four active legs			The passive leg		
3	UPS (PUS or RUS)		(Pa)PU	4-UPS&1-(Pa)PU	As shown in Fig. 2.38a
4			(Pa)RU	4-UPS&1-(Pa)RU	As shown in Fig. 2.38b
5			(Pa)S	4-UPS&1-(Pa)S	
6			P(Pa)U	4-UPS&1-P(Pa)U	
7			(Pa)UP	4-UPS&1-(Pa)UP	
8			R(Pa)U	4-UPS&1-R(Pa)R	

Where *P* prismatic joint, *R* revolute joint, *U* universal joint, (*Pa*) parallelogram, *S* spherical joint

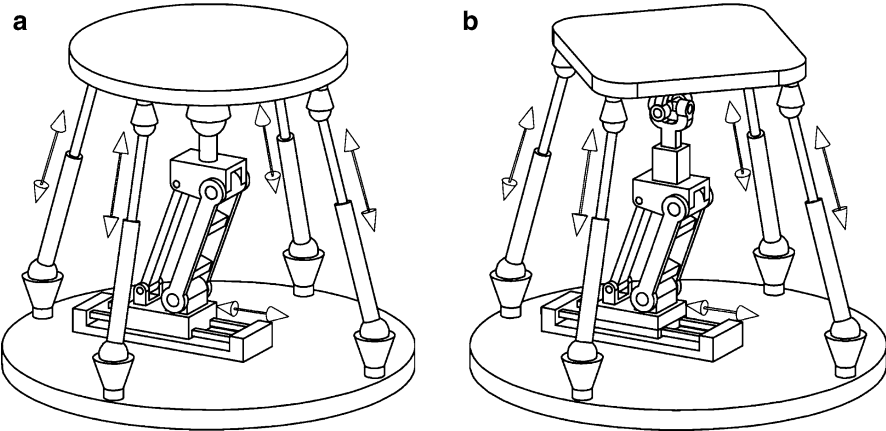


**Fig. 2.39** Two kinds of new 5-DOF parallel mechanisms: (a) with a 4-SPS&1-P(Pa)S chain and (b) with a 4-SPS&1-P(Pa)PU chain

parallelogram concept is also used in the design of such mechanisms. Application examples are TURIN (Sorli et al. 1997) with a 3-(Pa)(Pa)PS chain and a mechanism with 3-R(Pa)S chain proposed by Ebert-Uphoff (1998).

In the present chapter, three types of 6-DOF parallel mechanisms with parallelograms are discussed (Fig. 2.40). The mechanism in Fig. 2.40a consists of three identical legs, which are PP(Pa)S chains. In each of the three legs, two prismatic joints are actuated. For each of the two mechanisms shown in Fig. 2.40b, c, the mobile platform is connected to the base through the three legs as well; the mechanisms are equipped with 2-DOF planar actuators. Compared with the 3-PPRS mechanism and others with planar actuators, these parallel mechanisms have a much higher tilting capability. Table 2.9 lists some 6-DOF parallel mechanisms.

**Table 2.8** Some five-DOF parallel mechanisms with a parallelogram in their legs

No.	Leg chains		Mechanism chains	Remarks
	Legs with identical kinematic chains	The fifth leg		
1	UPS (PUS or RUS)	P(Pa)S	4-UPS&1-P(Pa)S	There are two cases: the actuated P joint can be vertical or horizontal. The vertical case is shown in Fig. 2.39a
2		P(Pa)PU	4-UPS&1-P(Pa)PU	There are two cases: the actuated P joint can be vertical or horizontal. The vertical case is shown in Fig. 2.39b
3		P(Pa)RU	4-UPS&1-P(Pa)RU	In the fifth leg, the P joint is actuated
4		P(Pa)UP	4-UPS&1-P(Pa)UP	In the fifth leg, the first P joint is actuated
5		(Pa)PS	4-UPS&1-P(Pa)S	In the fifth leg, the P joint is actuated
6		(Pa)RS	4-UPS&1-(Pa)RS	In the fifth leg, one of the four revolute joints in the parallelogram is actuated
7		R(Pa)S	4-UPS&1-R(Pa)S	In the fifth leg, the R joint is actuated

### 2.3.2 Type Synthesis Based on the Evolution Method

Many parallel mechanisms can be proposed using different methods. To a certain extent, these parallel mechanisms can provide inspiration for the design of potential new mechanisms. The modified mechanism may have relative advantages and good industrial applicability. In this section, we introduce some novel *3-DOF parallel mechanisms* that evolved from others.

Some spatial 3-DOF fully parallel mechanisms were introduced in section “3-DOF parallel mechanisms” (Figs. 2.30, 2.31, 2.32, 2.33, 2.34, and 2.35). In these mechanisms, at least one leg consists of a parallelogram. The parallelogram eventually presents difficulties in manufacturing and assembly as well as affects the accuracy and application of the mechanisms. These issues motivate us to identify a solution to overcome these problems.

As discussed in Sect. 4.1, the use of a parallelogram in each mechanism shown in Figs. 2.30, 2.31, 2.32, 2.33, 2.34, and 2.35 guarantees the unique rotational DOF of the mobile platform. For example, the parallelogram in a mechanism can restrict the rotations about the  $z$ - and  $x$ -axes (Fig. 2.30). The translation in the  $O$ - $yz$  plane of the mobile platform is implemented by actuating the sliders of the two legs (denoted as the first and second legs) with identical kinematic chains. The two legs are in the same plane, i.e., the  $O$ - $yz$  plane. Therefore, the leg with a parallelogram (referred to as the third leg) provides the mobile platform with the active rotation about the axis parallel to the  $y$ -axis and the passive translations along the  $x$ -,  $y$ -,

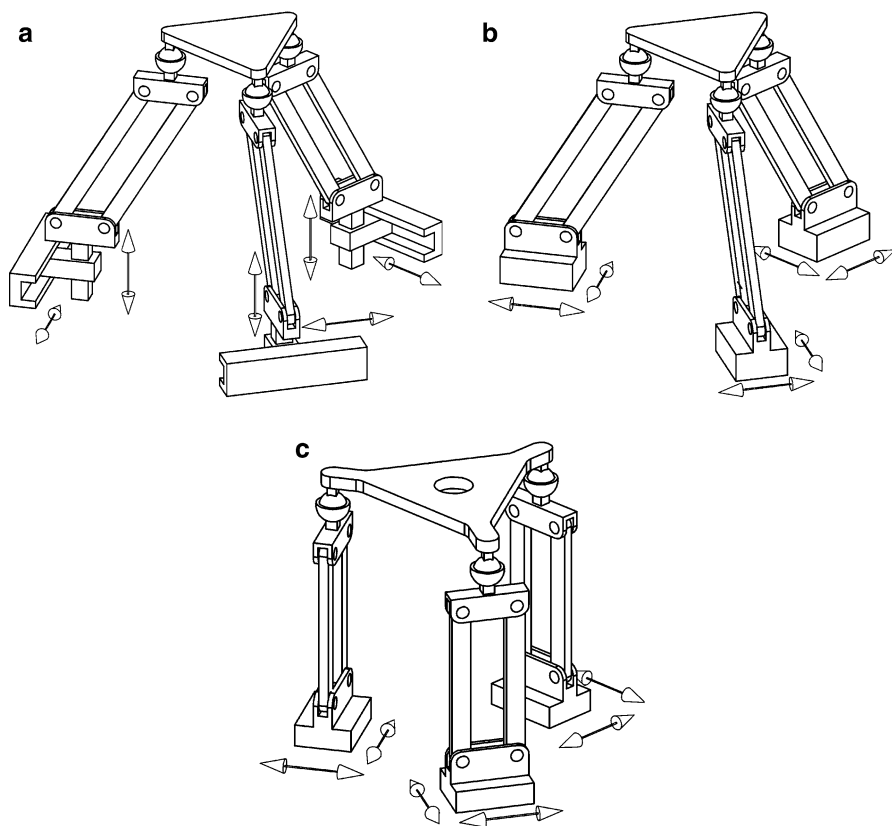


**Fig. 2.40** Three new types of 6-DOF parallel mechanisms

and  $z$ -axes. The translation along the  $x$ -axis is a parasitic motion. Observing the mechanism shows that at any position  $(y, z)$  of the mobile platform, the movement of the mobile platform and third leg is actually that of a slider-crank mechanism. If the  $z$ -coordinate of the mobile platform is specified, the change in shape of the parallelogram in the third leg conforms to the translation along the  $y$ -axis. Thus, replacing the third leg of the parallel mechanism with a PRC kinematic chain is feasible. The modified parallel mechanism is shown in Fig. 2.41a. In the new mechanism, legs 1 and 2 have identical kinematic chains, i.e., PRU (U-universal) chains. A U joint is usually composed of two R joints. In the two U joints, the axes of the two R joints that are connected to the mobile platform should be collinear. Otherwise, the mobile platform loses one DOF. Because of the PRC chain of leg 3, the two U joints can be replaced by two S (spherical joint) joints. Undoubtedly, the new mechanism also has the same DOFs as that of the mechanism shown in Fig. 2.30, i.e., the translation in the  $O$ - $yz$  plane and the rotation about the axis parallel to the  $y$ -axis if the P joints are actuated.

**Table 2.9** Some six-DOF parallel mechanisms with a four-bar parallelogram

Leg chains			Mechanism chains	Remarks
No.	First leg	Second leg		
1	PP(Pa)S	PP(Pa)S	3-PP(Pa)S	As shown in Fig. 2.40a
2	(PA) <sub>2</sub> (Pa)S	(PA) <sub>2</sub> (Pa)S	3-(PA) <sub>2</sub> (Pa)S	As shown in Fig. 2.40b
3	(PA) <sub>2</sub> (Pa)S	(PA) <sub>2</sub> (Pa)S	3-(PA) <sub>2</sub> (Pa)S	As shown in Fig. 2.40c

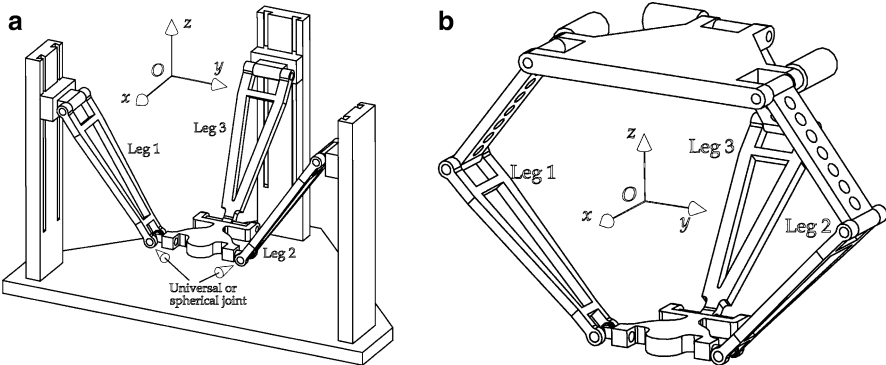


**Fig. 2.41** Modified parallel mechanisms of the mechanism shown in Fig. 2.30: (a) with linear actuators and (b) with revolute actuators

Although they have the same output, a huge difference in the kinematic motion of the third leg exists between the old and modified mechanisms. When the  $z$ -coordinate of the mobile platform is specified but the platform translates along the  $y$ -axis, the slider in the third leg of the old mechanism must be active accordingly to maintain the orientation of the platform. On the other hand, the slider in the new mechanism must be locked, indicating that the translation along the  $y$ -axis and rotation of the modified mechanism are decoupled. This also means that the mechanism is energy saving. Input error must exist in the actuator. Therefore, the active input in the mechanism in Fig. 2.30 may lead to the rotational error of the mobile platform. Thus, the difference enables the mechanism in Fig. 2.41a to accuracy that is better than that of the old mechanism. Additionally, the kinematic problem of the new mechanism is accordingly simpler (see the example in Sect. 3.8).

The modified parallel mechanism is clearly more complex than the old mechanism because the parallelogram is not used in the latter. In a planar parallelogram, every two links should be parallel to each other. This parallelism requires manufacturing accuracy and increases the difficulty of link machining and assembly, as well as costs. No parallelogram is used in the third leg; thus, the architecture of the new mechanism is simpler. The manufacturing is also easier, and the cost accordingly reduced. As shown in Fig. 2.41a, self-calibration can be implemented by attaching the sensors to the two revolute joints and cylinder joints that are connected to the mobile platform. Hereby, the accuracy of the modified parallel mechanism can be



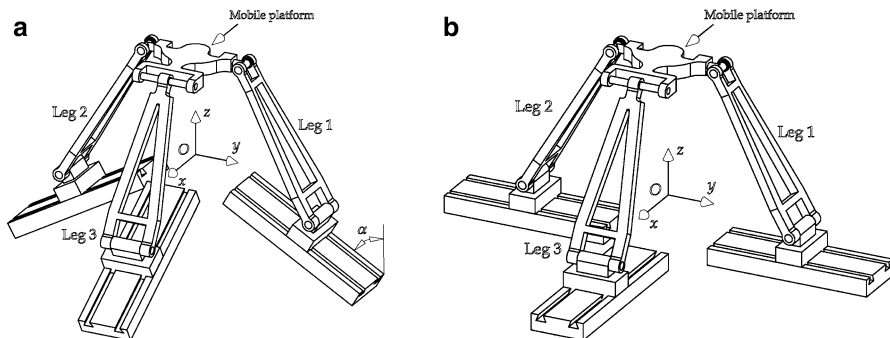


**Fig. 2.42** Modified parallel mechanisms: (a) with inclined angle  $\alpha$  and (b) with horizontal actuators

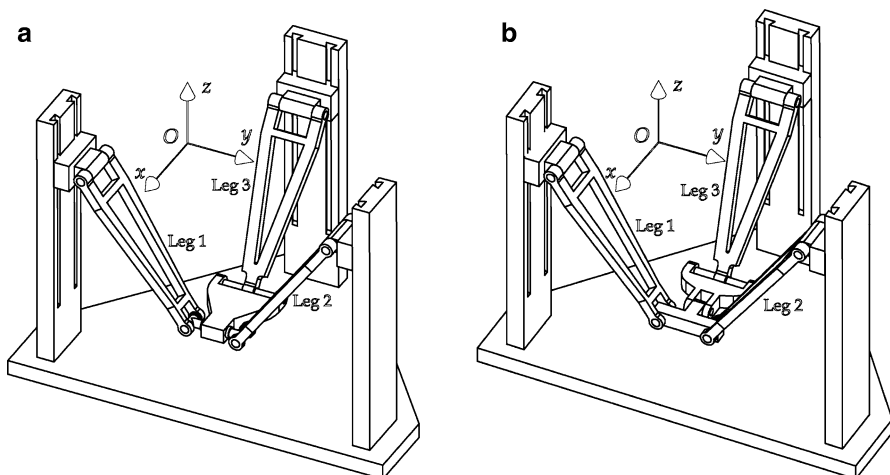


**Fig. 2.43** Modified parallel mechanism with a  $(PRR)_2R$ -PRC chain

improved. Compared with the old version, therefore, the new mechanism will be more popular in practical applications.

Figure 2.41b shows the modified parallel mechanism with revolute actuators, wherein the R joints fixed to the base are active. Notably, the actuation direction of all the sliders in the parallel mechanism shown in Fig. 2.41a with prismatic actuators may be inclined at an  $\alpha$  angle with respect to the vertical line (Fig. 2.42a). Figure 2.42b illustrates a typical example at a horizontal actuation direction.

Accordingly, kinematic chain  $(PRR)_2R\&PR(Pa)R$  of the parallel mechanisms shown in Fig. 2.32 may be replaced by the  $(PRR)_2R$ -PRC chain (see Fig. 2.43a). This modification, which has no negative influence on the kinematics and rotational capability of the mechanism, can be also extended to the parallel mechanism with revolute actuators (Fig. 2.43b). In the modified parallel mechanisms, the universal joints connected to the mobile platform can be replaced by spherical joints.

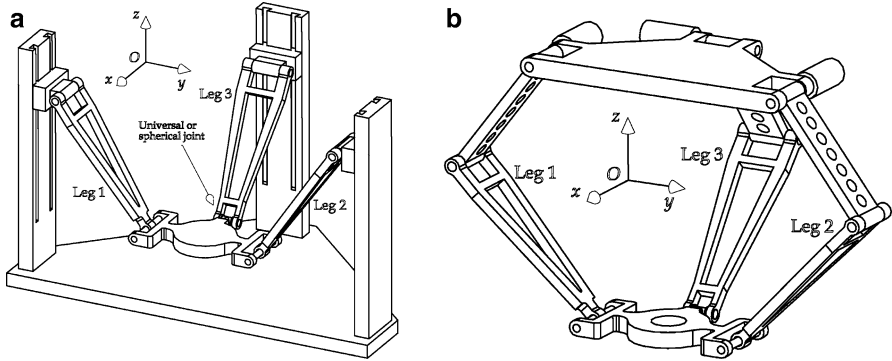


**Fig. 2.44** Modified parallel mechanisms of those shown in Fig. 2.31: (a) with linear actuators and (b) with revolute actuators

In the mechanism in Fig. 2.33a, two legs (the first and second legs) consist of a parallelogram. The kinematic chain of each of the two legs is the same as that of the third leg in the parallel mechanism shown in Fig. 2.30. Therefore, the two legs can also be replaced by the PRC chain. The new version of the parallel mechanism is illustrated in Fig. 2.44a. The new mechanism with revolute actuators is shown in Fig. 2.44b, in which the R joints fixed to the base platform are active.

As shown in Fig. 2.44a, the mobile platform of the mechanism is connected to the base by a PRU or PRS chain (leg 3) and two PRC chains (legs 1 and 2). The axes of the two C joints in legs 1 and 2 must be parallel to each other. If leg 3 uses the PRU chain, the axes must also be parallel to the R joint of the U joint that is connected to the mobile platform. Given the arrangement of the links and joints of the mechanism, the combination of the three legs constrains the rotation of the mobile platform with respect to the  $y$ - and  $z$ -axes and the translation along the  $y$ -axis, leaving the mechanism with two translational DOFs in the  $O$ - $xz$  plane and one rotational DOF about the axis parallel to the  $x$ -axis.

Similarly, the actuation direction of all the sliders in the parallel mechanism shown in Fig. 2.44a may be inclined at an  $\alpha$  angle with respect to the vertical line (Fig. 2.45a). Figure 2.45b illustrates a typical example at a horizontal actuation direction. They have the same mobility as the mechanism shown in Fig. 2.44a.

Compared with the mechanisms shown in Fig. 2.33, the parallel mechanisms introduced here also present advantages in terms of kinematics, architecture, manufacturing, energy cost, accuracy, and assembly for similar reasons.

No planar parallelogram is used in each mechanism of the new family; thus, every leg can be designed as a telescopic link. The parallel mechanisms with such links are shown in Fig. 2.46.

Although the modified mechanisms have some comparative advantages over the old parallel mechanisms, they are still characterized by disadvantages. For example, the adoption of the C joint may cause operational failure because it is a passive

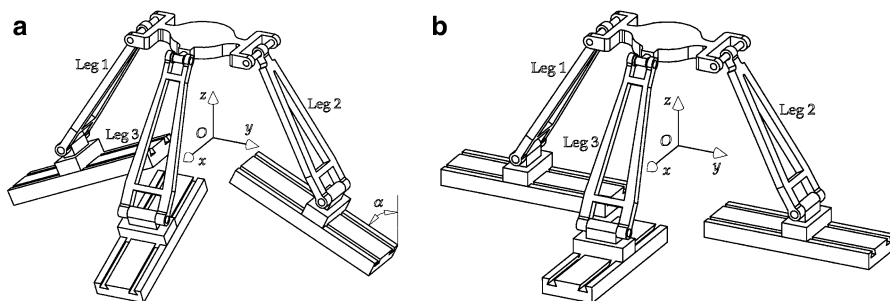


**Fig. 2.45** Modified parallel mechanisms: (a) with inclined angle  $\alpha$  and (b) with horizontal actuators

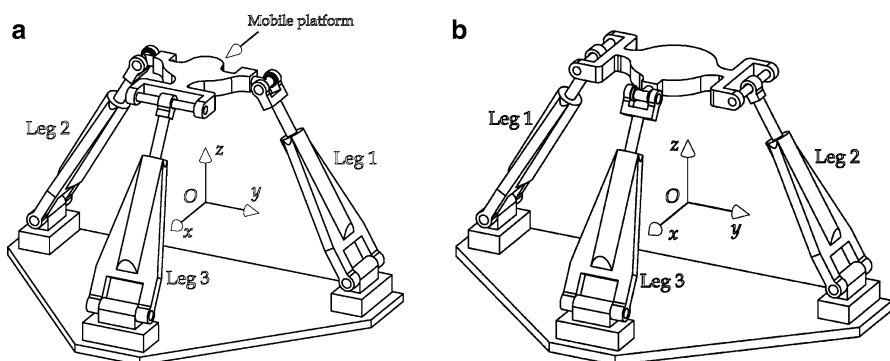


**Fig. 2.46** Modified parallel mechanisms with telescopic legs

joint. To avoid this problem, we can apply the passive DOF to the mechanisms. In the mechanisms shown in Fig. 2.41, for example, the joints connected to the mobile platform in the first and second legs can be spherical joints. In each of the spherical joints, one redundant DOF exists. A redundant R joint may also be added to the third leg of the mechanism in Fig. 2.41. On the other hand, to decrease the operational failure, the demand for parallelism of the C axes in the first and second legs should be very high.

The mechanism shown in Fig. 2.41a shows that with the C joint connected to the mobile platform, the translation along the y-axis is limited. If the C joint is excessively long, it will exhibit poor stiffness. Additionally, enhancing the accuracy of a C joint is usually a difficult task. Therefore, we can split the C joint into two joints, i.e., one R joint and one P joint, and move the P to the position near the base. The modified mechanism with a 2-PRRR&1-PPRR chain is shown in Fig. 2.47. With this change, both the stiffness and accuracy increase. Such a change can be realized in other mechanisms.

**Fig. 2.47** 2-PRRR&1-PPRR mechanism

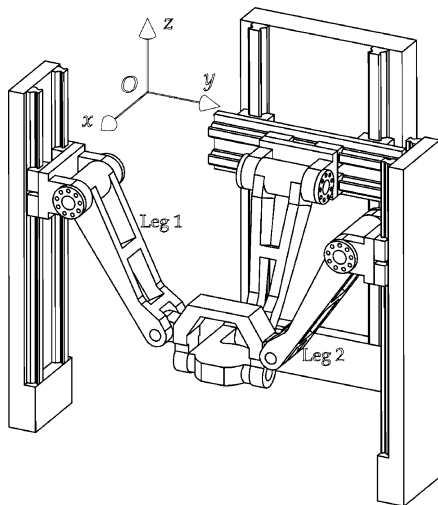
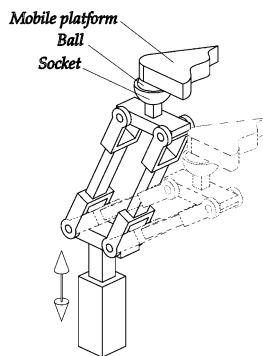


**Fig. 2.48** One leg of the 3-[PP]S parallel mechanism shown in Fig. 2.26d, in which the leg changes its configuration and the socket of the spherical joint maintains its orientation



The 3-[PP]S parallel mechanism shown in Fig. 2.28d illustrates that in each leg, the center point of the spherical joint moves in a plane and the socket link maintains its orientation when the leg changes its configuration because of the use of the parallelogram (Fig. 2.48). Consequently, the tilting capability of the mobile platform improves. The output link of a prismatic joint can retain its orientation. We consider replacing the parallelogram with a combined link and P joint. Such a mechanism is called a 3-PPS parallel mechanism. Figure 2.49a shows a general architecture for this type of mechanism, in which the angle from the horizontal line to the direction of the first P joint is  $\alpha'$ ,  $\alpha$  is the angle between the directions of the two P joints, and  $|\alpha - \alpha'| \neq 90^\circ$ . We assume that in each leg, the prismatic joint nearest the base would be actuated. Such a joint is denoted as the first P joint; meanwhile, another prismatic joint is referred to as the second P joint. Given that a 3-PPS mechanism can move vertically and the second prismatic joint is not actuated, the direction of the joint cannot be vertical. The 3-PPS mechanism can be modified into a 3-PCU mechanism because a cylinder joint is kinematically identical to the combined prismatic and revolute joint. For example, the 3-PPS mechanism at

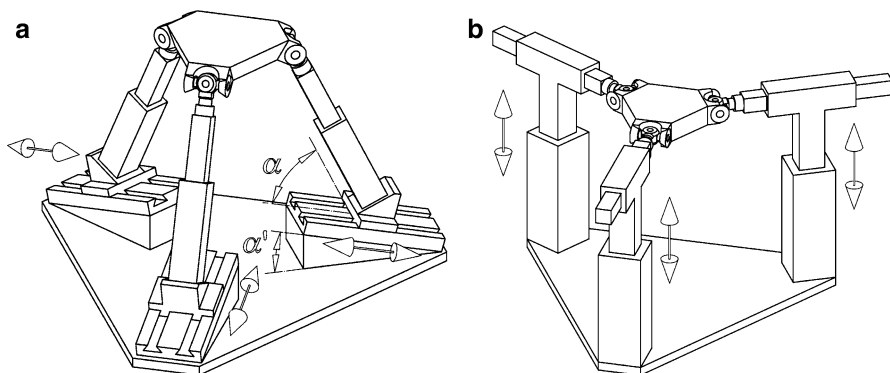
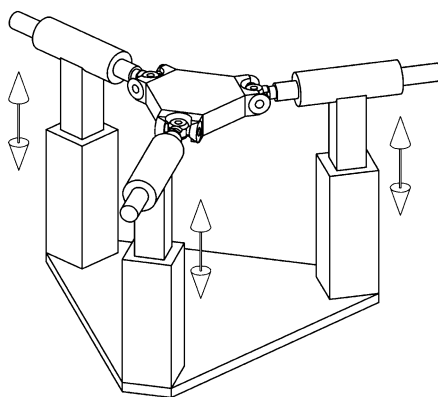


**Fig. 2.49** 3-PPS parallel mechanisms: (a) in a general architecture (b) in a special case,  $\alpha = \alpha' = 90^\circ$

**Fig. 2.50** 3-PCU parallel mechanism



$\alpha = \alpha' = 90^\circ$  (Fig. 2.49b) is identical to the 3-PCU mechanism shown in Fig. 2.50. The mechanism was proposed and analyzed in Liu et al. (2004). As analyzed in Liu and Bonev (2008), compared with the 3-PRS mechanism shown in Fig. 1.21, the 3-PPS mechanism in Fig. 2.49b exhibits a comparatively stable performance within its entire workspace. Generally, the parallel mechanism whose actuation directions are identical has an advantage in terms of direction, i.e., its performance is the same along that direction (Liu et al. 2006). Therefore, the 3-PPS and 3-PCU mechanisms in Figs. 2.49b and 2.50 are usually desirable.

## References

- Ball RS (1990) A treatise on the theory of screws. Cambridge University Press, Cambridge
- Carricato M, Parenti-Castelli V (2003) A family of 3-DOF translational parallel manipulators. ASME J Mech Des 125(2):302–307
- Ceccarelli M (1997) A new 3 D.O.F. spatial parallel mechanism. Mech Mach Theory 32(8): 895–902

- Chung Y-H, Lee J-W (2001) Design of a new 2 DOF parallel mechanism. In: Proceedings of IEEE/ASME international conference on advanced intelligent mechatronics, IEEE press, Piscataway, N.J., Como, pp 129–134
- Dafaoui E-M, Amirat Y, Pontnau J, Francois C (1998) Analysis and design of a six-DOF parallel mechanism, modeling, singular configurations, and workspace. *IEEE Trans Robot Autom* 14(1):78–92
- Dai JS, Huang Z, Lipkin H (2006) Mobility of overconstrained parallel mechanisms. *ASME J Mech Des* 128:220–229
- Ebert-Uphoff I, Gosselin CM (1998) Kinematic study of a new type of spatial parallel platform mechanism. In: Proceedings of DETC ASME design engineering technical conferences, Atlanta, Georgia, DETC/MECH-5962, ASME press, New York
- Fang Y, Tsai L-W (2002) Structure synthesis of a class of 4-DOF and 5-DOF parallel manipulators with identical limb structures. *Int J Robot Res* 21(9):799–810
- Frisoli A, Salsedo F, Bergamasco M (1999) Design of a new tendon driven haptic interface with six degrees of freedom. In: Proceedings of IEEE international workshop on robot and human interaction, IEEE press, Piscataway, N.J., Pisa, pp 303–308
- Gogu G (2005) Mobility of mechanisms: a critical review. *Mech Mach Theory* 40:1068–1097
- Hervé JM (1999) The Lie group of rigid body displacements, a fundamental tool for mechanism design. *Mech Mach Theory* 34(5):719–730
- Honegger M, Brega R, Schweitzer G (2000) Application of a nonlinear adaptive controller to a 6 dof parallel manipulator. In: Proceedings of IEEE international conference on robotics & automation, IEEE press, Piscataway, N.J., San Francisco, CA, pp 1930–1935
- Huang T, Li M, Zhao XM et al (2005a) Conceptual design and dimensional synthesis for a 3-DOF Module of the TriVariant—a novel 5-DOF reconfigurable hybrid robot. *IEEE Trans Robot* 21(3):449–456
- Huang T, Wang ZX, Li M, et al (2005b) A 3-DOF pure translational parallel mechanism with asymmetrical architecture. China Patent, No. 03144282.X
- Huang T, Zhao X, Whitehouse DJ (2002) Stiffness estimation of a tripod-based parallel kinematic machine. *IEEE Trans Robot Autom* 18(1):50–58
- Huang Z, Li QC (2002) General methodology for the type synthesis of lower-mobility symmetrical parallel mechanisms and several novel mechanisms. *Int J Robot Res* 21(2):131–145
- Huang Z, Li QC (2003) Type synthesis of symmetrical lower mobility parallel mechanisms using the constraint-synthesis method. *Int J Robot Res* 22(1):59–79
- Hudgens J, Tesar D (1988) A fully-parallel six degree-of-freedom micromanipulator: kinematics analysis and dynamic model. In: Proceedings of 20th Biennial ASME mechanisms conference, ASME press, Kissimmee, Florida, New York, pp 29–38
- Hunt KH (1978) Kinematic geometry of mechanisms. Clarendon Press, Oxford
- Kim W-K, Lee J-Y, Yi BJ (1997) Analysis for a planar 3 degree-of-freedom parallel mechanism with actively adjustable stiffness characteristics. In: Proceedings of IEEE international conference on robotics and automation, IEEE press, Piscataway, N.J., New Mexico, pp 2663–2670
- Kong X, Gosselin CM (2004a) Type synthesis of 3-DOF translational parallel manipulators based on screw theory. *ASME J Mech Des* 126(1):83–92
- Kong X, Gosselin CM (2004b) Type synthesis of 3T1R 4-DOF parallel manipulators based on screw theory. *IEEE Trans Robot Autom* 20(2):181–190
- Kutzbach K (1933) Einzelfragen Aus Dem Gebiet Der Maschinenteile. *Zeitschrift der Verein Deutscher Ingenieur* 77:1168–1169
- Lerbet J (1987) Mécanique des systèmes de solides rigides comportant des boucles fermées. Ph.D thesis, Paris VI, Paris
- Liu X-J (2001) Mechanical and kinematics design of parallel robotic mechanisms with less than six degrees of freedom. Post-Doctoral research report, Tsinghua University, Beijing (in Chinese)
- Liu X-J, Wang J, Gao F, Wang L-P (2001a) On the analysis of a new spatial three degrees of freedom parallel manipulator. *IEEE Trans Robot Autom* 17(6):959–968

- Liu X-J, Wang J, Wang L-P, Gao F (2001b) On the design of 6-DOF parallel micro-motion manipulators. In: Proceedings of the IEEE/RSJ international conference on intelligent robots and systems, IEEE press, Piscataway, N.J., Maui, Hawaii, pp 343–348
- Liu X-J, Bonev IA (2008) Orientation capability, error analysis, and dimensional optimization of two articulated tool heads with parallel kinematics. *ASME J Manuf Sci Eng* 130(1), Article Number: 011015
- Liu X-J, Pruschek P, Pritschow G (2004) A new 3-DOF parallel mechanism with full symmetrical structure and parasitic motions. In: Proceedings of international conference on intelligent manipulation and grasping, IEEE press, Piscataway, N.J., Genoa, pp 389–394
- Liu X-J, Tang X, Wang J (2005a) HANA: a novel spatial parallel manipulator with one rotational and two translational degrees of freedom. *Robotica* 23(2):257–270
- Liu X-J, Wang J (2003) Some new parallel mechanisms containing the planar four-bar parallelogram. *Int J Robot Res* 22(9):717–732
- Liu X-J, Wang J (2005) Some new spatial 3-DOF fully-parallel robotic mechanisms with high or improved rotational capability. In: Liu JX (ed) *Robots manipulators: new research*. Nova Science Publishers, New York, pp 33–64
- Liu X-J, Wang J, Pritschow G (2005b) A new family of spatial 3-DOF fully-parallel manipulators with high rotational capability. *Mech Mach Theory* 40(4):475–494
- Liu X-J, Wang Q-M, Wang J (2005c) Kinematics, dynamics and dimensional synthesis of a novel 2-DOF translational manipulator. *J Intell Robot Syst* 41(4):205–224
- Liu X-J, Wang J, Kim J (2006) Determination of the link lengths for a spatial 3-DOF parallel manipulator. *J Mech Des* 128:365–373
- Meng J, Liu G, Li Z (2007) A geometric theory for analysis and synthesis of sub-6 DOF parallel manipulators. *IEEE Trans Robot* 23(4):625–649
- Merlet J-P (2000) *Parallel robots*. Kluwer Academic Publishers, Dordrecht, pp 15–49
- Ohya Y, Arai T, Mae Y et al (1999) Development of 3-DOF finger module for micro manipulation. In: Proceedings of the 1999 IEEE/RSJ international conference on intelligent robots and systems, IEEE press, Piscataway, N.J., Kyongju, pp 894–899
- Pernette E, Clavel R (1996) *Parallel robots and microrobotics*. In: ISRAM'96, Montpellier, ASME press, New York, pp 535–542
- Pierrot F, Dauchez P, Fournier A (1991) Towards a fully-parallel 6 d.o.f. robot for high speed applications. In: Proceedings of IEEE international conference on robotics & automation, Sacramento, IEEE press, Piscataway, N.J., CA, pp 1288–1293
- Rico JM, Aguilera LD, Gallardo J et al (2006) A more general mobility criterion for parallel platforms. *ASME J Mech Des* 128:207–219
- Sorli M, Ferraresi C, Kolarski M et al (1997) Mechanics of TURIN parallel robot. *Mech Mach Theory* 32(1):51–57
- Tahmasebi F (1992) Kinematic synthesis and analysis of a novel class of six-DOF parallel minimanipulators. Ph.D thesis, University of Maryland, College Park
- Wang J, Gosselin CM (1999) Static balancing of spatial three-degree-of-freedom parallel mechanisms. *Mech Mach Theory* 34:437–452
- Yang T-L (2004) *Topology structure design of robot mechanisms* (in Chinese). China Machine Press, Beijing
- Zhao TS (2000) Some theoretical issues on analysis and synthesis for spatial imperfect-DOF parallel robots (in Chinese). Ph.D thesis, Yanshan University, Qinhuangdao
- Zhang D, Gosselin C M (2002) Kinetostatic analysis and design optimization of the Tricept machine tool family. *ASME J Manuf Sci Eng* 124(3):725–733

Parallel Kinematics

Type, Kinematics, and Optimal Design

Liu, X.-J.; Wang, J.

2014, XIII, 309 p.,

ISBN: 978-3-642-36929-2